© 2014. Published by The Company of Biologists Ltd | Journal of Cell Science (2014) 127, 1712–1725 doi:10.1242/jcs.134734

RESEARCH ARTICLE

SNARE-dependent interaction of Src, EGFR and β_1 integrin regulates invadopodia formation and tumor cell invasion

Karla C. Williams and Marc G. Coppolino*

ABSTRACT

Acquisition of an invasive phenotype is prerequisite for tumor metastasis. Degradation of the extracellular matrix (ECM), and subsequent invasion by tumor cells, is mediated, in part, through subcellular structures called invadopodia. Src-dependent cytoskeletal rearrangements are required to form invadopodia, and here we identify an association between Src, epidermal growth factor receptor (EGFR), and β1 integrin that facilitates invadopodia formation. The association of Src, EGFR and β1 integrin is dependent upon membrane traffic that is mediated by syntaxin13 (officially known as STX12) and SNAP23; a similar dependence on these two SNARE proteins was observed for invadopodium-based matrix degradation and cell invasion. Inhibition of SNARE function impaired the delivery of Src and EGFR to developing invadopodia, as well as the β1-integrin-dependent activation of Src and phosphorylation of EGFR on Tyr residue 845. We also identified an association between SNAP23 and β1 integrin, and inhibition of β1 integrin increased this association, whereas the interaction between syntaxin13 and SNAP23 was reduced. The results suggest that SNARE-dependent trafficking is regulated, in part, by β1 integrin and is required for the delivery of Src and EGFR to sites of invadopodia formation in order to support tumor cell invasion.

KEY WORDS: EGFR, SNARE, Src, Integrin, Invadopodia

INTRODUCTION

In multicellular organisms, movement of cells through the extracellular matrix (ECM) is an essential component of many physiological and pathological processes. Migration through an ECM requires cells to degrade ECM components, and in invasive tumor cells this is initiated by small subcellular structures called invadopodia (Murphy and Courtneidge, 2011; Yamaguchi et al., 2005). Invadopodia are F-actin-driven membrane protrusions that contain both receptors for ECM adhesion (integrins) and ECM-degrading proteolytic enzymes (matrix metalloproteases, MMPs). Invadopodia have been studied in cancer cells using two- and three-dimensional cell culture models, and evidence from *in vivo* studies supports the physiological importance (Soriano et al., 1991) and role in tumor progression (Blouw et al., 2008; Clark et al., 2009; Weaver, 2008) of invadopodia.

The formation of invadopodia is dependent upon remodeling of the F-actin-based cytoskeleton, which is regulated by Arp2/3 and neural Wiskott-Aldrich syndrome protein (N-WASP) (Yamaguchi et al., 2005). Src kinase has been shown to regulate cytoskeletal remodeling during invadopodia formation through phosphorylation of cortactin and Tks5 (tyrosine kinase substrate with five SH3 domains, also known as SH3PXD2A), and these substrates have established roles in invadopodia formation. Cortactin has been well characterized in this context and is known to modulate the actin cytoskeleton in association with Arp2/3 and N-WASP (Artym et al., 2006; Tehrani et al., 2007) as well as regulate the secretion of MMPs at invadopodia (Clark et al., 2007). Dephosphorylation of Src at Tyr527, and subsequent autophosphorylation at Tyr418, is required for modulation of the actin cytoskeleton, which frees the Src homology 3 and 2 domains (SH3 and SH2, respectively) to bind to, and facilitate the phosphorylation of, cortactin. Overexpression of Src frequently occurs in tumors, and the current study aimed to understand better how Src activity is regulated during invadopodia formation.

There is evidence that integrins and growth factor receptors play important roles in invadopodia formation and function. αvβ3 and β1 integrins have been found in invadopodia, and antibody-induced activation of β1 integrin increases degradation of the ECM (Mueller and Chen, 1991; Nakahara et al., 1998; Zambonin-Zallone et al., 1989). Loss of β1 integrin inhibited the formation of podosomes in osteoclasts and of invadopodia in Src-transformed fibroblasts (Destaing et al., 2010). Thus, it has been proposed that integrins contribute to invadopodia structure and function; however, their role in the formation of invadopodia has not been defined. Invadopodia formation can also be stimulated through epidermal growth factor (EGF) and platelet-derived growth factor (PDGF) receptor tyrosine kinases (RTKs) (Eckert et al., 2011; Mader et al., 2011). Interestingly, these studies have found that activation of RTKs increases the phosphorylation of cortactin and promotes the remodeling of F-actin at invadopodia.

Vesicular trafficking of invadopodium-associated proteins is a possible point of regulation in the formation of invadopodia. A protein family that has a major role in vesicle-mediated trafficking, soluble N-ethylmaleimide-sensitive factor attachment protein receptors (SNAREs), functions to localize vesicles to target membranes, and evidence supports a role for SNAREs in the transport of membrane type 1 MMP (MT1-MMP, also known as MMP14) during the maturation of invadopodia (Steffen et al., 2008). Here, we examine the role of SNARE-mediated trafficking during the progression of invadopodia formation and report that the inhibition of SNAREs disrupts the formation and maturation of invadopodia. The epidermal growth factor receptor (EGFR), Src and β1 integrin were found to associate, in a manner that was dependent upon the function of SNAREs [SNAP23 and syntaxin13 (officially known as STX12)], resulting in the phosphorylation of the EGFR at tyrosine residue 845 (Tyr845) independently of external growth factors. The interaction of syntaxin13 with SNAP23

Department of Molecular and Cellular Biology, University of Guelph, Guelph, ON N1G 2W1, Canada.

*Author for correspondence (mcoppoli@uoguelph.ca)

Received 8 May 2013; Accepted 16 January 2014

Journal of Cell Science

Journal of Cell Science (2014) 127, 1712–1725 doi:10.1242/jcs.134734

was regulated by β1 integrin, and knockdown of β1 integrin perturbed invadopodia-mediated ECM degradation and cell invasion. These observations point to novel roles for both the activation of β1 integrin and the SNARE-mediated trafficking of Src in the early stages of invadopodia formation. The results further suggest a mechanism by which Src might regulate invasive behavior in tumor cells that express high levels of Src and the EGFR.

RESULTS

Inhibition of syntaxin13 or SNAP23 impairs invadopodia formation and cell invasion

Previous studies have implicated SNARE-mediated trafficking, of MT1-MMP for example, in the process of tumor cell invasion (Steffen et al., 2008; Williams and Coppolino, 2011). To define the function of SNAREs during the invasion process, we examined the formation of invadopodia using a standard invadopodia formation assay (Artym et al., 2009). In this assay, invasive cell types, such as the MDA-MB-231 human mammary tumor cells used here, form invadopodia (marked by F-actin, cortactin and Src) after plating onto gelatin (supplementary material Fig. S1). SNARE function was inhibited by transiently transfecting cells with a dominant-negative form (E329Q-NSF) of the enzyme N-ethylmaleimide-sensitive factor (NSF), an ATPase that is required for the activity of SNAREs (Skalski et al., 2011; Whiteheart et al., 1994). Cells expressing E329Q-NSF failed to form punctae containing both F-actin and cortactin (supplementary material Fig. S2), suggesting that SNARE-mediated membrane trafficking is involved in the early stages of invadopodia formation. In order to determine which SNARE proteins were mediating the formation of actin–cortactin punctae, we transfected cells with inhibitory SNARE constructs and assessed the formation of F-actin–cortactin punctae (Fig. 1A). We targeted syntaxin13 and SNAP23 because these SNAREs have been previously described to have roles in ECM degradation and cell invasion (Kean et al., 2009), and we speculated that they might be involved in the formation of invadopodia. The isolated cytoplasmic domain of syntaxin13 (syntaxin13cyto) can form complexes with endogenous SNARE binding partners, which blocks the interactions with cognate SNARE partners and exerts a dominant-negative effect (Collins et al., 2002). SNAP23 lacking its C-terminal nine amino acids (SNAP23CΔ9) forms nonfunctional complexes that are unable to support membrane fusion (Huang et al., 2001). Constructs of this type have been used extensively to inhibit SNARE function in several experimental systems (Collins et al., 2002; Hirling et al., 2000; Huang et al., 2001; Kean et al., 2009; Mallard et al., 2002; Polgár et al., 2002; Scott et al., 2003; Skalski et al., 2010; Williams and Coppolino, 2011; Xu et al., 2002).

Inhibition of syntaxin13 or SNAP23 reduced the formation of punctae that contained both F-actin and cortactin (Fig. 1A,D). By contrast, inhibition of the SNAREs VAMP3 or GS15 (also known as BET1L) had no effect (Fig. 1A,C). Reductions in the formation of invadopodia were also observed when SNARE expression was decreased using siRNA to target syntaxin13 or shRNA to target SNAP23 (Fig. 1A,B,D). The effects of inhibiting syntaxin13 and SNAP23 were similar to the effects of general inhibition of the function of SNAREs using dominant-negative NSF (supplementary material Fig. S1); therefore, we focused our investigations on these two SNAREs.

To determine whether perturbation of the function of F-actin–cortactin punctae was affecting the maturation of invadopodia into degradative structures, we quantified matrix degradation using a quantitative fluorescent-matrix degradation assay (Artym et al., 2009). Inhibition of SNAP23 or syntaxin13, or RNAi-mediated knockdown of SNAP23 or syntaxin13, reduced degradation of the matrix by more than 75% (Fig. 1E,G). Accordingly, inhibition of either SNAP23 or syntaxin13 also reduced cell invasion by 79%±4.5 and 67%±6.8 (±s.e.m.), respectively, in Matrigel-based invasion assays (Fig. 1F). Furthermore, RNAi-mediated knockdown of SNAP23 or syntaxin13 also potently impeded cell invasion (Fig. 1F). Because long-term inhibition of SNAP23 is potentially lethal to cells, we assessed cell viability (using Trypan Blue exclusion) during inhibition of SNAP23 (20 h post-transfection) and shRNA-mediated knockdown of SNAP23 (72 h post-transfection), and found no significant effect (96%±7.4 and 92%±9.1, respectively). These results indicate that the functions of SNAP23 and syntaxin13 are required for normal formation and maturation of invadopodia into degradative structures and for cell invasion.

Syntaxin13- and SNAP23-mediated trafficking of Src is required for invadopodia formation

During the formation of invadopodia in MDA-MB-231 cells, F-actin punctae containing Src and cortactin formed at the ventral cell membrane, ~40 min after plating cells onto gelatin (supplementary material Fig. S1B). Src-mediated phosphorylation of cortactin can initiate F-actin polymerization and invadopodia formation (Tehrani et al., 2007), and we observed changes to the distribution of Src in cells in which SNARE-mediated trafficking had been inhibited (supplementary material Fig. S1C). In control cells, Src was found to colocalize with syntaxin13 at intracellular compartments, and SNAP23 was found to colocalize with Src at the plasma membrane (Fig. 2A). The plasma membrane was identified by transfecting cells with a construct that encoded the acylation motif of Lyn kinase fused to the green fluorescent protein (GFP) (Teruel et al., 1999). Inhibition of either syntaxin13 or SNAP23 significantly reduced the amount of Src at the plasma membrane (Fig. 2A,B). These findings suggest that the activities of syntaxin13 and SNAP23 are required for the trafficking of Src.

In an effort to restore invadopodia formation, either wild-type Src (Src-WT) or a constitutively membrane-targeted form of Src (Src-CAAX) was co-transfected with plasmids to inhibit SNARE function, and the formation of invadopodia was analyzed. Src-CAAX contains the CAAX domain from K-Ras and has been shown previously to rescue the effects of mislocalized Src (Skalski et al., 2011). Overexpression of Src-WT or Src-CAAX increased the average number of punctae containing both F-actin and cortactin in cells compared with controls; however, there was no significant difference between the number of F-actin–cortactin punctae formed by cells that overexpressed Src-WT compared with Src-CAAX (Fig. 2C,D). Importantly, expression of Src-CAAX, but not Src-WT, partly restored the formation of punctae containing both F-actin and cortactin in cells that expressed either SNAP23CΔ9 or syntaxin13cyto, or in cells with RNAi-mediated knockdown of SNARE expression (Fig. 2A,E,F). There was a general trend showing a slight reduction of F-actin–cortactin punctae in cells that expressed Src-CAAX and either SNAP23CΔ9 or syntaxin13cyto compared with cells that expressed the Src-CAAX control. This suggests that SNAP23 and syntaxin13 are involved in trafficking other invadopodium proteins that contribute to stabilization and maturation of the F-actin core. Similar effects were observed in another carcinoma cell line, HT1080 (supplementary material Fig. S3A,B). Taken

Journal of Cell Science (2014) 127, 1712–1725 doi:10.1242/jcs.134734

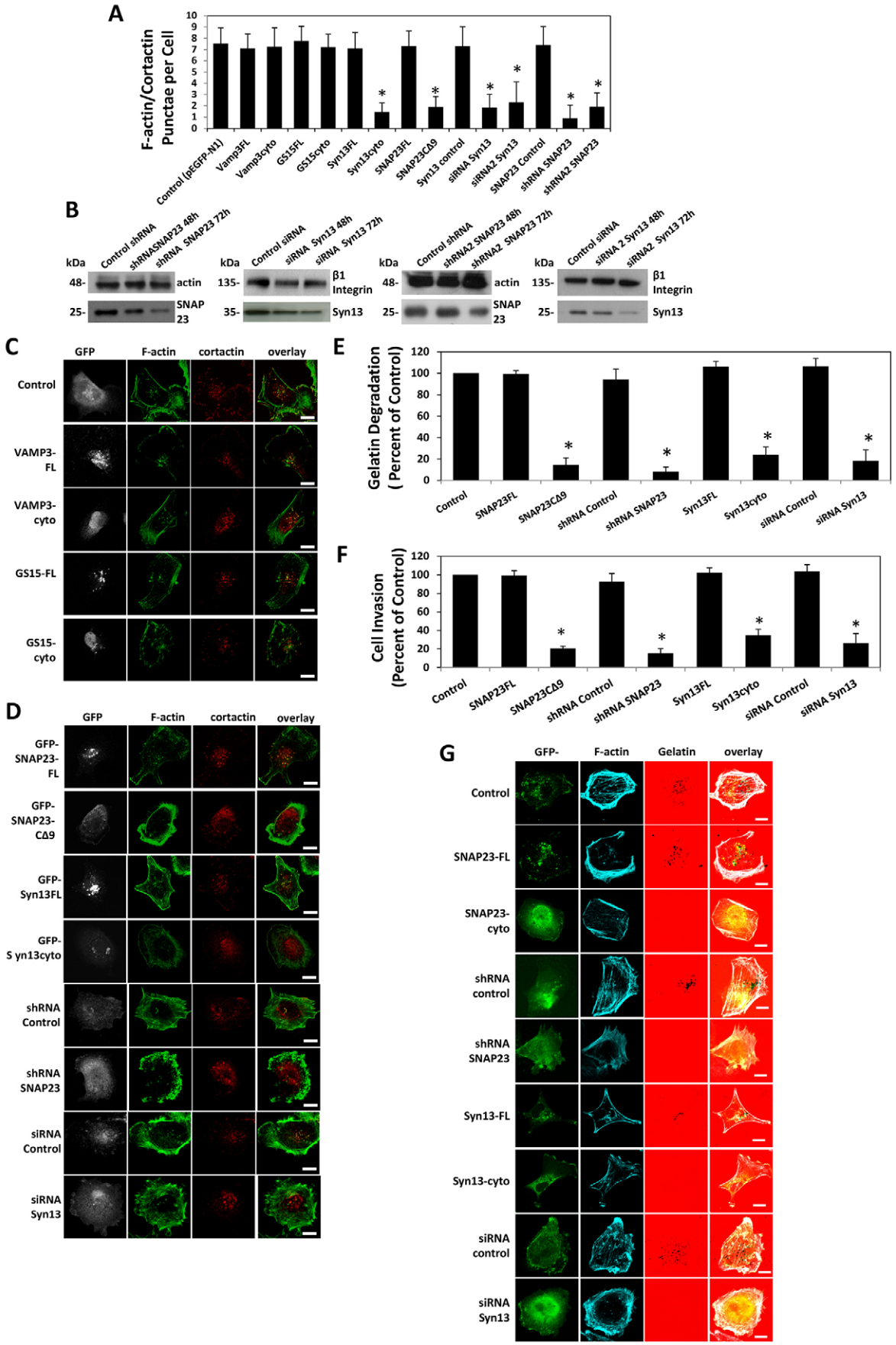

Fig. 1. See next page for legend.

Journal of Cell Science (2014) 127, 1712–1725 doi:10.1242/jcs.134734

Fig. 1. SNAP23 and syntaxin13 **are required for invadopodia formation, ECM degradation and cell invasion.** Cells were transfected with GFP, or GFP-tagged constructs of VAMP3 [the full-length (FL) protein or the inhibitory cytoplasmic domain (cyto)], syntaxin13 (syn13; FL or cyto), GS15 (FL or cyto), SNAP23 (FL) or the inhibitory SNAP23 protein (CΔ9). Alternatively, cells were transfected with siRNA against syntaxin13, siRNA control, shRNA to SNAP23 or shRNA control. (A) Cells were serum-starved overnight, plated onto gelatin-coated coverslips for 40 min (serum-free), fixed, permeabilized and stained for cortactin and F-actin (phalloidin). The number of F-actin–cortactin punctae per cell was then counted. Means±s.e.m. are shown from three independent experiments in which 30–50 cells per sample were analyzed. (B) Knockdown of SNAP23 and syntaxin13 at 48 h and 72 h by using two different siRNA or shRNA constructs. β1 integrin and actin represent loading controls. (C,D) Cells that had been transfected were fixed, permeabilized and stained for cortactin and F-actin (phalloidin). (E,G) Cells that had been transfected were plated on Alexa-Fluor-594-labeled gelatin, fixed, permeabilized and stained for F-actin. Cells with F-actin punctae that overlay black spots of matrix degradation were counted as cells that form active invadopodia. Means±s.e.m. are shown from three independent experiments in which 100 cells per sample were counted. (F) Cells that had been transfected were subjected to Transwell insert invasion assays. Cells that had invaded through Matrigel towards 10% FBS for 18 h were fixed and counted. Means±s.e.m. from three independent experiments are shown. *$P<0.05$, values significantly different from wild-type cells. Scale bars: 10 μm.

together, the findings suggest that syntaxin13 and SNAP23 are required for the trafficking of Src during the formation of invadopodia.

Src phosphorylates EGFR in a SNARE-dependent manner

The effect that targeting Src to the plasma membrane had on invadopodia formation led us to explore the mechanism through which Src was acting. Invadopodia formation has been shown to involve signaling through growth factor receptors, including the EGFR (Mader et al., 2011), which is a known target for Src-mediated phosphorylation. Src-mediated phosphorylation of the EGFR on Tyr845 has previously been shown to regulate the proliferation and transformation of breast cancer cells (Mueller et al., 2012; Sato et al., 2003); therefore, we assessed the localization of Src and the EGFR during invadopodia formation and examined the phosphorylation of the EGFR on Tyr845. When serum-starved cells were plated onto a gelatin matrix, Src and the EGFR were observed to colocalize at the ventral membrane of cells 20 min after plating; furthermore, Src, the EGFR and F-actin were colocalized together at immature invadopodia at 40 min after plating (Fig. 3A). Quantification of the colocalization of Src and the EGFR by using data taken from multiple cells from replicate experiments revealed 66.29%±14.92 (±s.e.m.) of pixels colocalized, with a Pearson's correlation of 0.94±0.06. Quantification of the colocalization of F-actin with Src or the EGFR indicated that 35.47%±9.96 and 39.20%±12.71 of pixels were colocalized with a Pearson's correlation of 0.91±0.1 and 0.89±0.07, respectively. It was also observed that Src and the EGFR colocalized with Tks5, another invadopodium marker, at 40 min (Fig. 3A) (61.79%±18.67 and 49.24%±15.02 of colocalized pixels, Pearson's correlations of 0.90±0.08 and 0.87±0.04, respectively). Phosphorylation of the EGFR on Tyr845 was detected in these F-actin punctae using an antibody specific to EGFR that had been phosphorylated at Tyr845 (Fig. 3B), and quantification of colocalization with F-actin revealed 48.89%±15.1 of pixels colocalized with a Pearson's correlation of 0.93±0.02 (Fig. 3B). Taken together, these results demonstrate that Src, the EGFR and EGFR that has been phosphorylated at Tyr845 localize to immature invadopodia structures.

Phosphorylation of the EGFR at 40 min after plating was detectable by western blot (Fig. 3C), and inhibition of Src activity using the Src inhibitor PP2 decreased this phosphorylation by greater than 80% (Fig. 3C,F). Expression of either SNAP23CΔ9 or syntaxin13cyto decreased phosphorylation of the EGFR on Tyr845 (Fig. 3D), and RNAi-mediated knockdown of either SNAP23 or syntaxin13 also reduced phosphorylation on both the EGFR at Tyr845 and Src at Tyr418 by greater than 60% (Fig. 3E,F). Inhibition of Src by using PP2, or inhibition of the EGFR by using AG1478, reduced by more than 60% matrix degradation (Fig. 3G,I) and reduced cell invasion by 64.4%±10.2 and 73%±11.2 (±s.e.m.) (Fig. 3H), respectively. These results are consistent with a requirement for the trafficking of Src to the plasma membrane, whereby Src is activated and subsequently phosphorylates the EGFR to promote invadopodia formation. Furthermore, it is apparent that the development of mature invadopodia, capable of measurable matrix degradation, is reduced when the activity of Src or the EGFR is inhibited.

Syntaxin13 and SNAP23 are involved in trafficking of EGFR to the plasma membrane

Observations that syntaxin13cyto and SNAP23CΔ9 reduced the formation of punctae containing both F-actin and cortactin, and decreased localization of Src at the plasma membrane and phosphorylation of the EGFR, suggest that these SNAREs are involved in the trafficking of Src and, possibly, the EGFR to the plasma membrane. Syntaxin13 colocalized with Src, the EGFR and Tks5 at ventral F-actin punctae 30 min after plating onto gelatin (Fig. 4A). Quantification of the colocalization of syntaxin13 with Src, the EGFR and Tks5 revealed that 46.25%±17.00, 43.9%±7.2 and 43.7%±14.5 of pixels colocalized (±s.e.m.), with Pearson's correlations of 0.94±0.10, 0.91±0.07 and 0.92±0.05, respectively. In cells transfected with syntaxin13cyto, minimal amounts of Src and the EGFR were observed at the ventral surface of cells, but both were found to colocalize in a large peri-nuclear compartment that was marked by Rab11 (Fig. 4A). The EGFR was also found to colocalize with SNAP23 and Tks5 at the ventral surface of cells (Fig. 4B) (SNAP23 with the EGFR: 47.9%±16.6 colocalized pixels, Pearson's correlation=0.93±0.08; SNAP23 with Tks5: 39.62%±6.5 colocalized pixels, Pearson's correlation=0.90±0.06). This suggests that syntaxin13 and SNAP23 might be involved in the targeting of the EGFR to invadopodial sites. Inhibition of SNAP23 or syntaxin13 significantly reduced the amount of EGFR that localized to the cell surface compared with either control (GFP) cells or cells transfected with GFP-tagged full-length syntaxin13 or SNAP23 (syntaxin13FL and SNAP23FL, respectively), indicating that the trafficking of the EGFR to the plasma membrane is dependent upon the function of these SNAREs (Fig. 4C–E).

The distributions of Src and the EGFR, and the reduction of Src and the EGFR at the plasma membrane that was caused by inhibition of syntaxin13 and SNAP23, suggest that Src and the EGFR might co-traffic to the plasma membrane, possibly as a complex. Therefore, co-immunoprecipitation experiments were performed, and an association between Src and the EGFR was detected that was found to be independent of Src activity (Fig. 4F,H). The association of Src with the EGFR was also detected in immunoprecipitates from cells transfected with syntaxin13FL, syntaxin13cyto, SNAP23FL or SNAP23CΔ9 (Fig. 4F–H). These findings suggest that Src and EGFR associate, independently of Src activity, before being trafficked to sites of invadopodia formation.

Journal of Cell Science (2014) 127, 1712–1725 doi:10.1242/jcs.134734

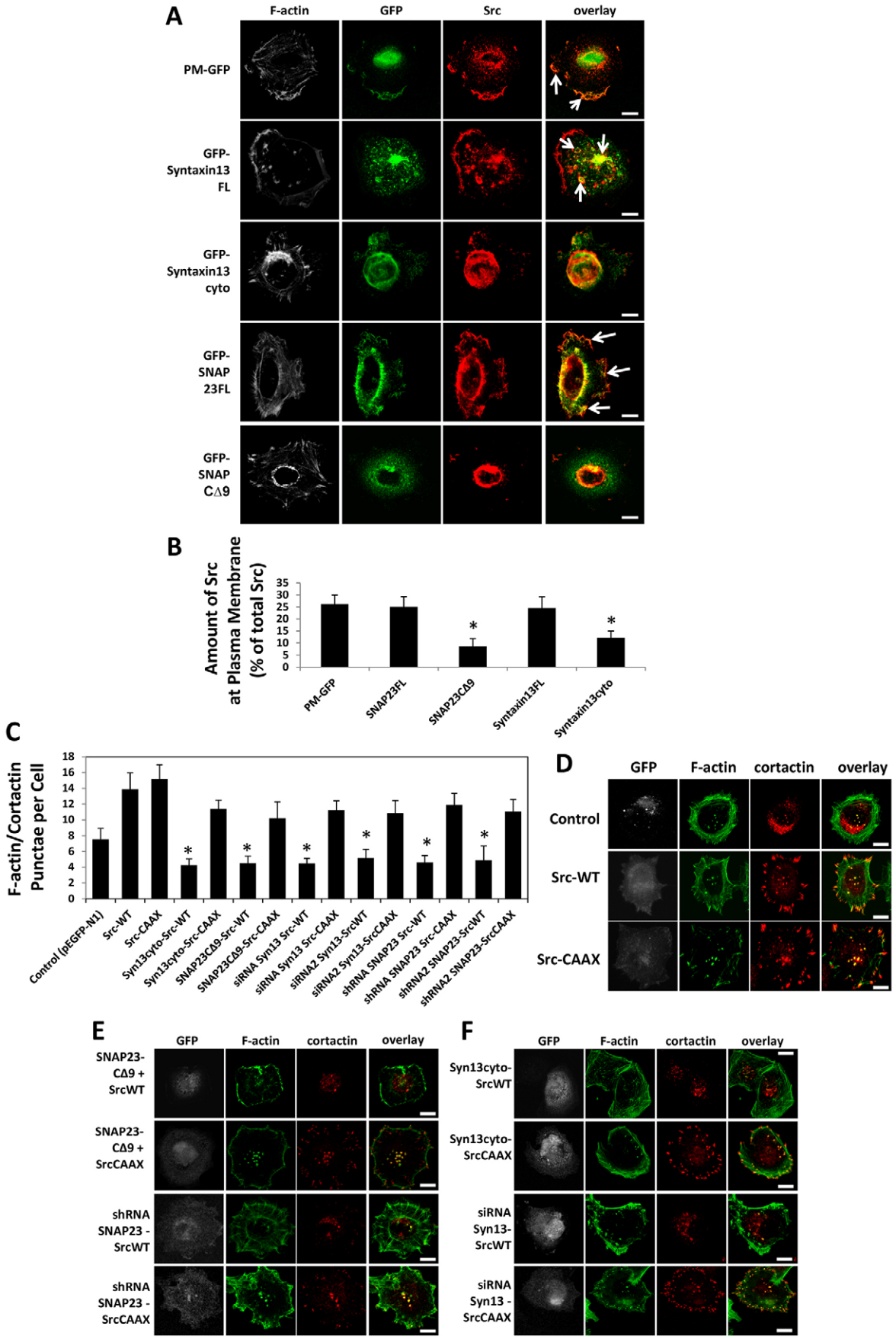

Fig. 2. See next page for legend.

Fig. 2. SNAP23 and syntaxin13 support Src-dependent invadopodia formation and Src trafficking. (A,B) Cells were transfected with either plasma-membrane-targeted GFP (PM-GFP), GFP–syntaxin13FL, GFP–syntaxin13cyto, GFP–SNAP23FL or GFP–SNAP23cΔ9. Cells were then fixed, permeabilized and stained for Src and F-actin (phalloidin). Stacks of confocal slices were acquired using constant parameters (*z* projections of entire stacks are shown). Arrows point to sites of colocalization of Src with the indicated constructs. (B) Quantification of plasma membrane Src using ImageJ and presented as a percentage of total Src. (C–F) Cells were co-transfected with Src-WT or Src-CAAX in combination with GFP or GFP-tagged constructs (full length or inhibitory, as described in Fig. 1) of SNAP23 or syntaxin13, or in combination with siRNA to syntaxin13, siRNA control, shRNA to SNAP23 or shRNA control. Cells were serum-starved overnight and plated onto gelatin-coated coverslips for 40 min (serum-free). Cells were then fixed, permeabilized and stained for cortactin and F-actin (phalloidin). (C) Quantification of the number of F-actin–cortactin punctae per cell. Means±s.e.m. are plotted from three independent experiments in which 30–50 cells per sample were analyzed. *$P<0.05$ denotes a value significantly different from that of cells expressing the corresponding full-length SNARE. (D–F) Cells expressing Src-WT or Src-CAAX together with GFP, GFP–SNAP23FL, GFP–SNAP23CΔ9, GFP–syntaxin13FL, GFP–syntaxin13cyto, siRNA control, siRNA against syntaxin13, shRNA control or shRNA against SNAP23 were imaged by using confocal microscopy. Images are single confocal slices of the ventral cell membrane of representative cells; the GFP signal is shown in the left column (gray). Invadopodia formation is represented by colocalization of F-actin (green) and cortactin (red) in the overlay (yellow and orange). Scale bars: 10 μm.

β1 integrin affects the interaction between SNAP23 and syntaxin13

The effect that the inhibition of syntaxin13 had on the trafficking of Src and the EGFR to the plasma membrane might mean that SNAP23 acts as a cognate SNARE for docking of syntaxin13. Consistent with this, we observed that SNAP23 and syntaxin13 colocalized with F-actin punctae at 30 min post-plating onto gelatin (Fig. 5A) (SNAP23 and syntaxin13: 78.68%±10.64 colocalized pixels, Pearson's correlation=0.94±0.04; SNAP23 or syntaxin13 colocalization with F-actin: 39.6%±13 and 33.7%±14.9 colocalized pixels, with Pearson's correlations of 0.91±0.07 and 0.82±0.10, respectively, ±s.e.m.). Co-immunoprecipitation experiments demonstrated that a complex containing SNAP23 and syntaxin13 was present at 20 min and 40 min after cells had been plated onto gelatin (Fig. 5B).

Given the recent findings that β1 integrins can affect trafficking of the EGFR (Caswell et al., 2008; Onodera et al., 2012) and invadopodia formation (Destaing et al., 2010), we hypothesized that β1 integrin might be influencing the association of syntaxin13 with SNAP23. To test this, we inhibited β1 integrin by treating cells with the β1-integrin-blocking antibody AIIB2 and then immunoprecipitated syntaxin13 from cell lysates. A reduction in the amount of SNAP23 that co-immunoprecipitated with syntaxin13 was observed when β1 integrin was inhibited (Fig. 5C), which indicates that β1 integrin activity influences SNARE complex formation. The possibility of an interaction between SNAP23 and β1 integrin, which could function to promote SNARE complex assembly, was then examined. β1 integrin was found to co-immunoprecipitate with SNAP23 at 20 min and 40 min after plating onto a gelatin matrix (Fig. 5D). This association was then examined in cells treated with the antibody AIIB2 or the β1-integrin-activating antibody P4G11. The actions of the β1-integrin-activating or -inhibiting antibodies were confirmed by monitoring phosphorylation of focal adhesion kinase (FAK) (Fig. 5F). An increase in the amount of β1 integrin that was pulled down with SNAP23 was observed in samples in which β1 integrin had been inhibited, whereas a decrease in this association was detected in samples in which β1 integrin had been activated (Fig. 5E). SNAP23 and syntaxin13 were also found to colocalize with β1 integrin and Tks5 at the ventral plasma membrane of cells that had been plated onto gelatin (Fig. 5G). Quantification of β1 integrin colocalization with Tks5, SNAP23 and syntaxin13 revealed 30.31%±9.67, 56.69%±9.70 and 51.19±15.8% of pixels colocalized, with Pearson's correlations of 0.85±0.06, 0.88±0.03 and 0.88±0.10, respectively (±s.e.m.). Along with the decreased association between SNAP23 and syntaxin13 that was caused by inhibition of β1 integrin, these observations suggest that activation of β1 integrin allows SNAP23 to form a SNARE complex with syntaxin13.

Src and the EGFR associate with β1 integrin in a SNARE-dependent fashion

It is possible that β1 integrin associates with Src and the EGFR in a complex, and, to test this, the EGFR was immunoprecipitated from cells, and co-immunoprecipitation of β1 integrin with Src was assessed (Fig. 6A–C). Src was readily co-immunoprecipitated with the EGFR from cells before plating (0 min), as well as at 20 and 40 min post-plating. β1 integrin was detected in association with the EGFR at 40 min after plating (Fig. 6A,F). The formation of this Src–EGFR–β1-integrin complex was dependent upon SNARE-mediated trafficking as the amount of β1 integrin that co-immunoprecipitated with Src and the EGFR was reduced in the lysate from cells transfected with SNAP23CΔ9, syntaxin13cyto, the shRNA to SNAP23 or the siRNA to syntaxin13 (Fig. 6B,C). Given that the localization of Src and the EGFR at the plasma membrane affects their amount of phosphorylation (Fig. 3F), we assessed whether β1 integrin activity could also affect their phosphorylation. Cells were treated with the β1 integrin inhibitory antibody AIIB2 and this led to reductions in Src phosphorylation on Tyr418 and EGFR phosphorylation on Tyr845 (Fig. 6D,E). These observations reveal that β1 integrin function is necessary for the activation of Src and the phosphorylation of the EGFR. The results are consistent with a model in which Src and EGFR are trafficked, as part of a complex, to the plasma membrane where Src can be activated, possibly by β1 integrin, and phosphorylate the EGFR. It was also observed in Src immunoprecipitates that the Src–EGFR–β1-integrin complex forms more quickly after plating (being detectable by 20 min) in the presence of serum (Fig. 6G) compared with serum-free conditions (Fig. 6F). This is possibly due to the increased turnover of focal adhesions and the EGFR at the plasma membrane in the presence of growth factors. Consistent with results obtained in the absence of serum (Fig. 3C and Fig. 6D), a reduction in the phosphorylation of EGFR at Tyr845 and of Src at Tyr418, resulting from inhibition of β1 integrin or Src, was also observed in the presence of serum (Fig. 6H). These results suggest a role for β1 integrin in the regulation of the phosphorylation of the EGFR by Src, possibly by binding to the Src–EGFR complex at the plasma membrane.

Analysis of the intracellular distribution of Src, EGFR and β1 integrin by microscopy revealed localizations of these proteins that were consistent with the results of the immunoprecipitations above. Single confocal slices revealed the distributions of EGFR, Src and β1 integrin at the ventral plasma membrane (Fig. 6I,J). At 20 min post-plating, Src and EGFR colocalize at small punctae with β1 integrin, this is consistent with the low amount of β1 integrin that was detected in the EGFR and Src immunoprecipitates at 20 min (Fig. 6A,F). At 40 min, Src and the EGFR colocalize with β1 integrin at larger punctae (Fig. 6I, bottom right overlay), and quantification of the colocalization

Journal of Cell Science (2014) 127, 1712–1725 doi:10.1242/jcs.134734

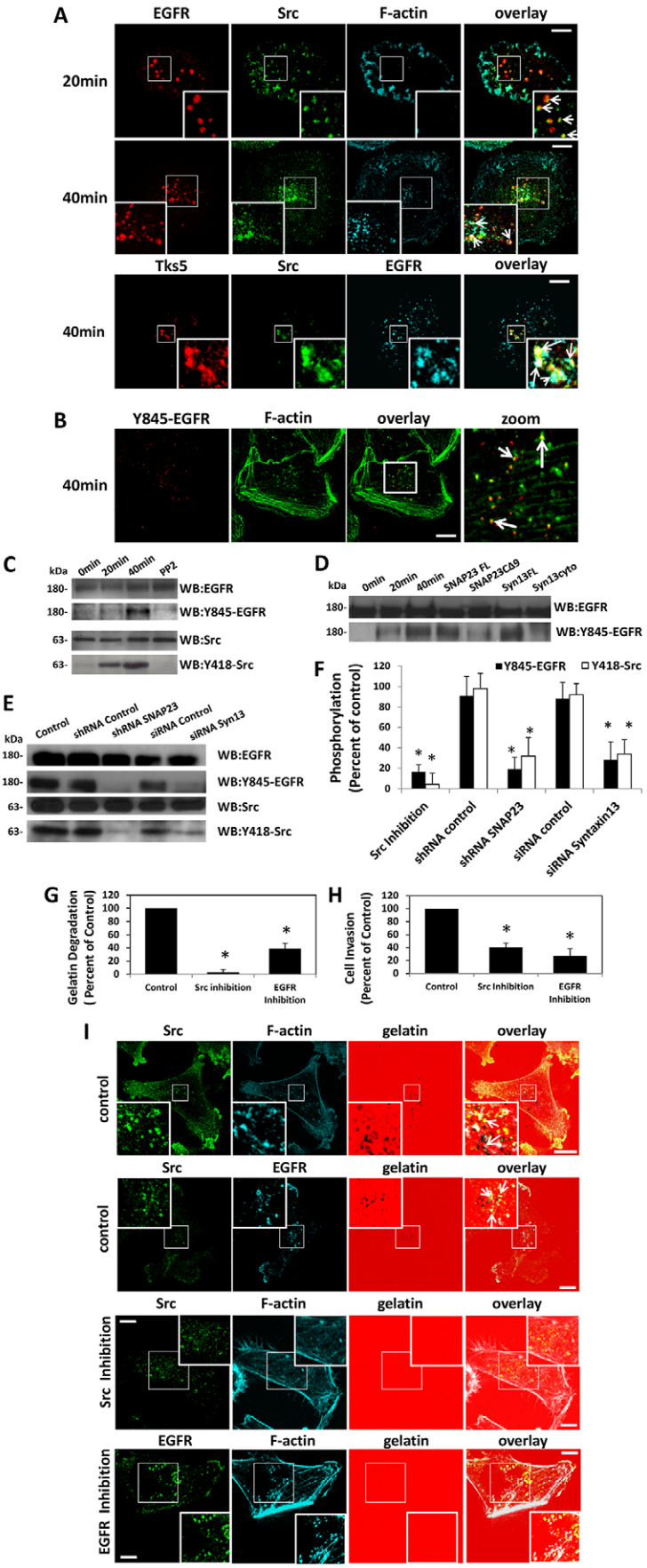

Fig. 3. The EGFR and Src localise to invadopodia and are phosphorylated in a SNARE-dependent manner. Serum-starved cells were plated onto gelatin for 40 min, unless otherwise indicated, followed by fixation (A,B) or lysed and subjected to SDS-PAGE and western blot (WB) analysis (C–F). Cells were stained for (A) the EGFR, Src and either F-actin or Tks5; or (B) the EGFR that had been phosphorylated at Tyr845 (Y845-EGFR) and F-actin. Confocal images of the ventral cell membrane are shown. (A) Top row: at 20 min, EGFR (red) and Src (green) colocalize at the ventral surface before formation of an F-actin core. Middle row: the EGFR and Src colocalize at ventral F-actin cores (cyan) at 40 min (white in overlay). Bottom row: the EGFR (cyan) and Src (green) colocalize with ventral Tks5 (red) at 40 min (white in overlay). (B) Y845-EGFR (red) colocalizes with F-actin punctae (green) at 40 min after plating onto gelatin. In A,B, arrows indicate sites of colocalization. (C) PP2 (10 μM, added at the time of plating) inhibits phosphorylation of Src and the EGFR. Membranes were probed for Y845-EGFR or Src that had been phosphorylated at Tyr418 (Y418-Src) (lower panel of each pair), stripped and then re-probed for the EGFR and Src (upper panels). (D) Inhibition of SNAREs by transfection of cells with indicated constructs reduces phosphorylation of the EGFR. The membrane was probed for Y845-EGFR (lower panel), and then stripped and re-probed for the EGFR (upper panels). (E) Knockdown of SNARE expression reduces phosphorylation of Src and the EGFR. Membranes were probed, as in A, for both total and phosphorylated levels of Src or the EGFR. (F) Quantification of Src and EGFR phosphorylation from western blots. The means±s.e.m. from three replicate experiments are shown. (G) Cells were plated on Alexa-Fluor-594-labeled gelatin and treated with 10 μM PP2 (Src inhibitor) or 11 nM AG1478 (inhibitor of the EGFR) for 3 h. Cells with F-actin punctae overlaying black spots of matrix degradation were counted as cells forming degradative invadopodia. The means±s.e.m. from three independent experiments in which 100 cells per sample are shown. (H) Cells were subjected to Transwell insert invasion assays. PP2, AG1478 or DMSO as a control were added at the time of plating. Cells that had invaded through the Matrigel towards 10% FBS for 18 h were then fixed and counted. In G,H, $*P<0.05$ denotes a value significantly different from that of control cells. Means±s.e.m. from three independent experiments are shown. (I) Cells were treated with PP2, AG1478 or DMSO as a control, plated on Alexa-Fluor-594-labeled gelatin, fixed, permeabilized and stained for Src, the EGFR, and/or F-actin, as indicated. Confocal slices of ventral membrane are shown. The insets show zoomed images of the boxed regions; arrows in the top two rows indicate sites of invadopodium-based gelatin degradation containing Src and F-actin or EGFR. Scale bars: 10 μm.

Journal of Cell Science

Journal of Cell Science (2014) 127, 1712–1725 doi:10.1242/jcs.134734

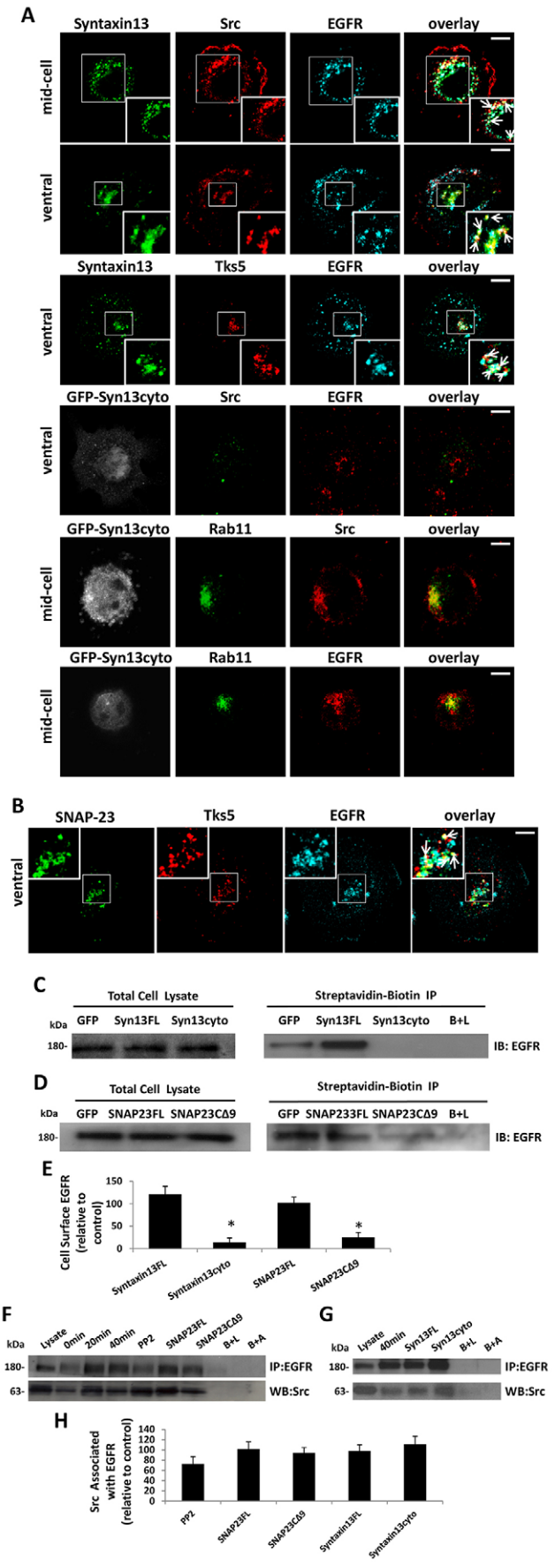

Fig. 4. Syntaxin13 and SNAP23 facilitate trafficking of the EGFR to the plasma membrane. Cells were transfected with GFP–Syntaxin13cyto or left untransfected, serum-starved and then plated onto gelatin. (A,B) Cells were fixed, permeabilized and then stained for syntaxin13, SNAP-23, Src, the EGFR, Tks5 or Rab11, as indicated. The distribution of proteins is shown in single confocal slices either through the middle of the cell (mid-cell) or at the ventral membrane (ventral), as specified. Insets show zoomed images of the boxed regions. Colocalization is seen as white in overlays and is indicated by arrows. Endogenous syntaxin13 and SNAP23 are shown except where the GFP-tagged construct is used (shown in gray). (C,D) Immunoprecipitates (IP) of cell surface proteins in cells that had been transfected with GFP–syntaxin13 constructs (FL or cyto) or GFP–SNAP23 constructs (FL or CΔ9). Left panels, 20 μg of total cell lysate; right panels, immunoprecipitates. Blots were probed for the EGFR (IB). (E) Quantification of cell surface EGFR. *$P<0.05$ denotes value significantly different from samples transfected with corresponding full-length SNARE construct. Mean±s.e.m. from three replicate western blots. (F,G) Immunoprecipitates of the EGFR were analysed by western blotting (WB) for the presence of Src and the EGFR. Cells that had been treated with PP2 (10 μM) or transfected with the indicated constructs were lysed at 40 min after plating onto gelatin. B+L, beads plus cell lysate; B+A, beads plus antibody. (H) Quantification of the amount of Src in EGFR immunoprecipitates Mean±s.e.m. from three replicate western blots. Scale bars: 10 μm (A,B).

revealed that 35.39%±7.90 and 39.4%±8.3 of pixels colocalized, with Pearson's correlations of 0.84±0.10 and 0.87±0.14, respectively (±s.e.m.). The colocalization of F-actin with the EGFR and β1 integrin at ventral punctae was obvious at 30 and 40 min after plating (Fig. 6J). Interestingly, at 30 min post-plating, colocalization of EGFR and β1 integrin with F-actin can be seen as ring-shaped structures (Fig. 6J, top right overlay, yellow arrows), as opposed to the more distinct punctae seen at 40 min (Fig. 6J, bottom right, white arrows). Quantification of β1 integrin colocalization with F-actin revealed that 41.3%±11.1 of pixels colocalized, with a Pearson's correlation of 0.91±0.07.

Knockdown of β1 integrin impairs invadopodium degradation and invasion

To examine the function of β1 integrin in invadopodium-based cell invasion, we used standard gelatin degradation and Matrigel invasion assays. Knockdown of β1 integrin expression by using shRNA (Fig. 7A) reduced the number of punctae containing both F-actin and cortactin (Fig. 7B,C) and significantly reduced invadopodium-based matrix degradation (Fig. 7D,F). shRNA-mediated knockdown of β1 integrin also reduced cell invasion by greater than 80% (Fig. 7E). Similar results were obtained in another carcinoma cell line, HT1080 (supplementary material Fig. S3H). Together, these results suggest that β1 integrin is involved in the formation of invadopodia and in cell invasion. Overall, the results of this study highlight the importance of β1 integrin, Src and EGFR activity during invadopodia formation and tumor cell invasion.

DISCUSSION

Invadopodia have been identified as key structures in tumor cells that facilitate the degradation of the ECM (Linder, 2007; Weaver, 2008), and here we have identified a SNARE-mediated trafficking pathway that controls the formation of invadopodia, assisted by the interaction of β1 integrin with a complex containing both Src and the EGFR. We propose a model wherein β1 integrin activity modulates the co-trafficking of Src with the EGFR, which is mediated through a SNARE complex containing syntaxin13 and SNAP23, to sites of cell–ECM attachment. Src and the EGFR associate with β1 integrin, resulting in Src activation and the subsequent phosphorylation

Journal of Cell Science

Journal of Cell Science (2014) 127, 1712–1725 doi:10.1242/jcs.134734

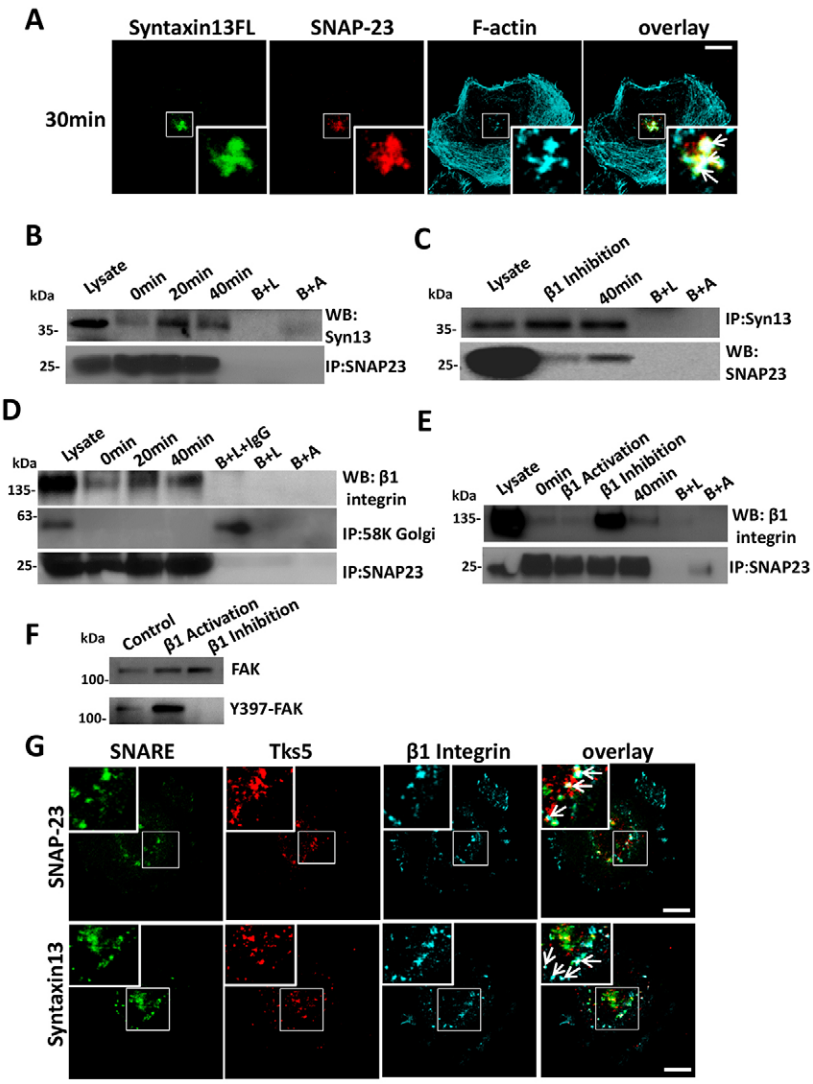

Fig. 5. The interaction between SNAP23 and syntaxin13 is stimulated by β1 integrin. (A) Cells were transfected with GFP–syntaxin13FL, plated onto gelatin for 30 min, fixed, permeabilized, stained with antibodies against SNAP23 and Alexa-Fluor-647–phalloidin, and then analyzed by using confocal microscopy. The insets show zoomed images of the boxed regions. Arrows point to areas of colocalization between syntaxin13, SNAP23 and F-actin.
(B–F) Immunoprecipitates (IP) from extracts of cells that had been treated as indicated. (B) SNAP23 was immunoprecipitated at the indicated time-points and probed for syntaxin13. (C) Syntaxin13 was immunoprecipitated from control cells or cells treated with the inhibitory antibody against β1 integrin. WB, western blot. (D,E) SNAP23 immunoprecipitates from cells under the indicated conditions were probed for β1 integrin. Control cell lysate (20 μg) was loaded into the first lane in B–E. B+L, beads plus cell lysate; B+A, beads plus antibody. B+L+IgG control (antibody against 58K Golgi protein) was loaded in D. (F) Lysates from control cells or from cells that had been treated with β1-integrin-activating or inhibitory antibody (10 μg/ml) were probed for FAK that had been phosphorylated at Tyr397 (Y397-FAK). Membranes were then stripped and re-probed for total FAK. (G) SNAP23 and syntaxin13 (green) colocalize with Tks5 (red) and β1 integrin (cyan) at the ventral membrane of cells (white in overlay). The inset shows zoomed images of the boxed regions. Arrows point to sites of colocalization. Scale bars: 10 μm.

of the EGFR, which stabilizes these sites for the recruitment of other proteins, and allows maturation of the invadopodia.

Our results are consistent with growing evidence that stimulation of growth factor receptors – such as the PDGF receptor, the hepatocyte growth factor receptor (MET) and the EGFR – induces invadopodium or podosome formation (Eckert et al., 2011; Mader et al., 2011; Rajadurai et al., 2012) through signaling pathways involving Src and protein kinase C. Src is known to promote invadopodium and podosome formation through stimulating the assembly of the F-actin core (Destaing et al., 2008) and has been shown to phosphorylate cortactin to enhance actin filament assembly (Tehrani et al., 2007). There is also evidence that integrins, including αvβ3 and β1 integrins, function at invadopodia (Desai et al., 2008; Destaing et al., 2010; Mueller and Chen, 1991; Nakahara et al., 1998); however, the role of integrins in invadopodia formation has not been thoroughly characterized. In the current study, we have observed Src localization at newly formed invadopodia and determined that invadopodium stabilization and maturation are dependent on β1 integrin activation and SNARE-mediated membrane trafficking of a Src–EGFR complex to sites of cell–ECM interaction.

An EGFR–Src–β1-integrin complex was found to associate with assembling F-actin core structures at the ventral cell membrane during the early stages of invadopodia formation. Inhibition of SNARE-mediated membrane trafficking reduced the interaction between the EGFR, Src and β1 integrin and decreased phosphorylation of the EGFR and Src. Src activity and subsequent EGFR phosphorylation in this context are dependent upon their localization at the plasma membrane, and we determined that inhibiting the trafficking of Src perturbed invadopodia formation, matrix degradation and cell invasion. The results and our proposed model clearly indicate the importance of Src translocation to the plasma membrane during the formation of invadopodia. During the trafficking of Src and the EGFR, SNAP23 formed a complex with syntaxin13, and these SNAREs colocalized at sites of F-actin core formation. Formation of this complex was impaired by inhibition of β1 integrin, and SNAP23 was found to associate with β1 integrin in a manner that was enhanced upon inhibition of β1 integrin. From this, we speculate that inactive β1 integrin interacts with SNAP23 and prevents formation of the SNARE complex. Upon β1 integrin activation, SNAP23 is released and is then able to bind syntaxin13.

Knockdown of β1 integrin reduced the formation of invadopodia that were capable of degrading the ECM. β1 integrin is known to regulate signaling pathways that involve phosphoinositide 3-kinase

Journal of Cell Science (2014) 127, 1712–1725 doi:10.1242/jcs.134734

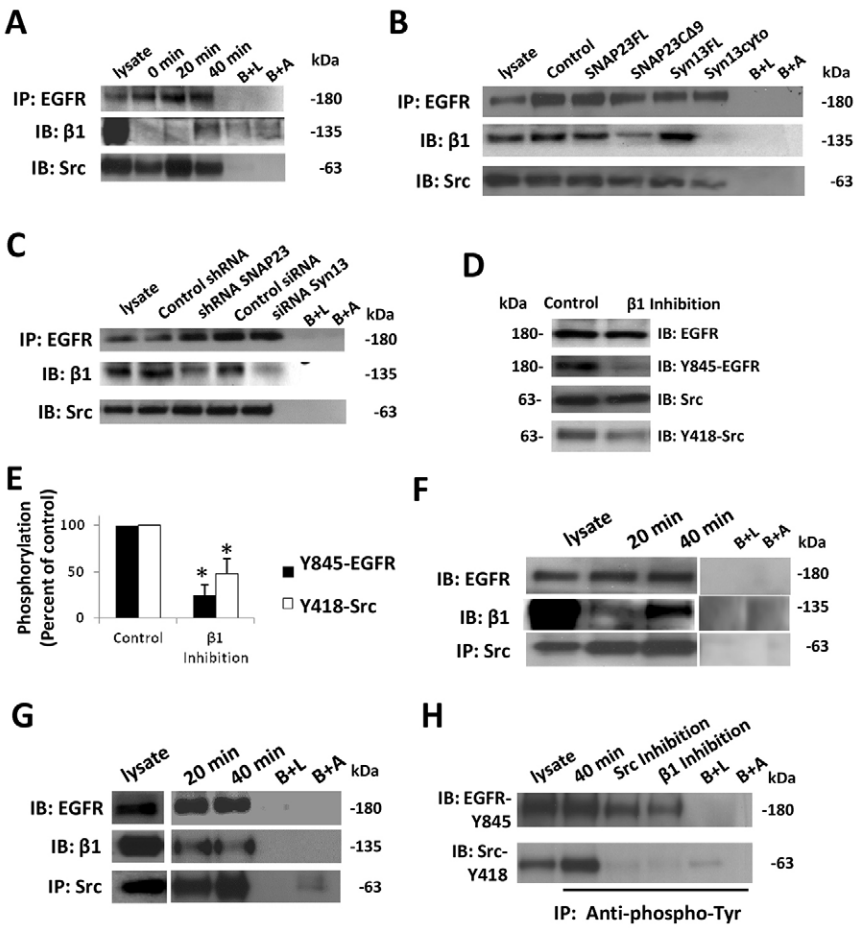

Fig. 6. Src, EGFR and β1 integrin associate and colocalize during the formation of invadopodia. Serum-starved cells were plated onto gelatin and extracted for immunoprecipitation (at 40 min after plating, unless specified otherwise). (A) EGFR immunoprecipitates (IP) were probed for Src, the EGFR and β1 integrin by western blotting (IB). B+L, beads plus cell lysate; B+A, beads plus antibody. (B,C) EGFR immunoprecipitates from cells transfected with the indicated constructs were probed for Src, EGFR and β1 integrin. (D) Total cell lysates from control cells or cells plated with inhibitory antibodies against β1 integrin were probed for the phosphorylated EGFR or Src (Y845-EGFR and Y418-Src, respectively). Membranes were then stripped and re-probed for total EGFR and Src. (E) Quantification of Src and EGFR phosphorylation. **P*<0.05 denotes xxxxxx. Mean±s.e.m. from three replicate western blots. (F,G) Src immunoprecipitates were probed for EGFR, Src and β1 integrin. Cells were grown in medium containing 10% FBS before plating onto gelatin under the indicated conditions. (H) Phospho-tyrosine immunoprecipitates were probed for Y845-EGFR and Y418-Src. Control cell lysate (20 μg) was loaded into the first lane in A–C and F–H. B+L, beads plus cell lysate; B+A, beads plus antibody. (I,J) Serum-starved cells were plated onto gelatin, fixed, permeabilized and then stained as indicated. Single confocal slices and zoomed images of the boxed regions (inset) from the ventral membrane are shown. (I) β1 integrin (cyan) colocalizes with Src (green) and EGFR (red) at 20, 30 and 40 min after plating (white in overlay). (J) β1 integrin (green) colocalizes with F-actin (cyan) and EGFR (red) (white in overlay). Arrows point to areas of colocalization. Scale bars: 10 μm.

Journal of Cell Science (2014) 127, 1712–1725 doi:10.1242/jcs.134734

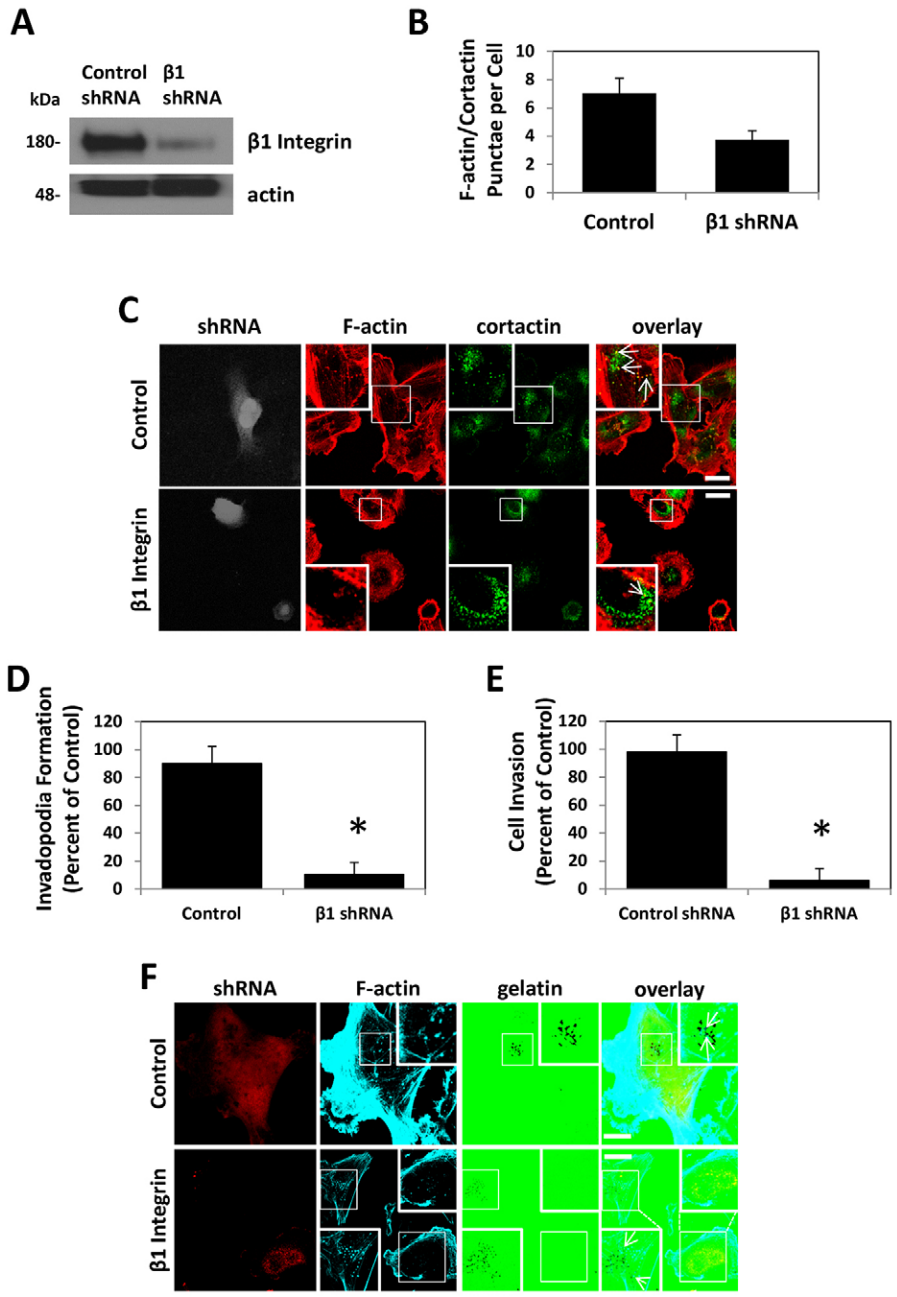

Fig. 7. Knockdown of β1 integrin impairs invadopodia formation and cell invasion. Cells were transfected with either control shRNA or shRNA against β1 integrin for 96 h. (A) Western blots of lysates from the transfected cells were probed for β1 integrin and actin. (B) Quantification of the number of punctae containing both F-actin and cortactin from cells that had been transfected. (C) Transfected cells were plated onto gelatin, fixed, permeabilized and stained for F-actin and cortactin. Zoomed images of the boxed regions are shown in the insets. Arrows indicate punctae containing both F-actin and cortactin. (D–F) Cells that had been plated on Alexa-Fluor-488-labeled gelatin for 3 h (D,F) or subjected to Transwell insert invasion assays for 18 h were fixed and then counted (E). The percentage of cells (relative to control), which had been transfected with control shRNA or shRNA against β1 integrin, that formed active invadopodia (D) or invaded through Matrigel was calculated (E). *$P<0.05$ denotes a value significantly different from control cells. Means±s.e.m. from three independent experiments are shown. (F) Images of F-actin punctae and the corresponding sites of gelatin degradation in control and β1-integrin-knockdown cells. Zoomed images of the boxed regions are shown in the inset. Arrows indicate degradative punctae in a control cell (top row), and in a non-transfected cell and a cell that had been transfected with shRNA against β1-integrin (bottom row). Scale bars: 10 μm.

(PI3K) and AKT (Velling et al., 2004), FAK (Wennerberg et al., 2000), as well as Src (Meng and Lowell, 1998). β1 integrin has also been shown to modulate expression of E-cadherin (Serio, 2012) and the integrins α6 and β4 (Huck et al., 2010). Alterations to these pathways might affect both invadopodia formation and cell invasion. Overall, the results suggest an important role for β1 integrin in the localization, organization and function of invadopodia and are consistent with studies demonstrating that β1 integrin stabilizes and regulates the assembly of invadosomes and invadopodia (Beaty et al., 2013; Destaing et al., 2010).

The EGFR is overexpressed in several invasive cancers, and its activation has been shown to stimulate tumor invasion and dissemination (Biscardi et al., 2000; Garouniatis et al., 2012; Kim and Muller, 1999). Tyr845 is the only tyrosine residue in the activation loop of the EGFR (Jorissen et al., 2003), and it was recently demonstrated that high levels of the EGFR that has been phosphorylated at Tyr845 can be found in some metastatic cancers (Aquino et al., 2012). Small-molecule inhibitors and monoclonal antibodies against the EGFR that block ligand-induced EGFR autophosphorylation have been developed for therapeutic use (O'Donovan and Crown, 2007; Dai et al., 2005; von Minckwitz et al., 2005), but our observations from experiments performed in the absence of growth factors suggest an important role for EGFR signaling, independent of binding to EGF, in tumor cell invasion. Phosphorylation of the EGFR, at Tyr845 can be stimulated by Src and β1 integrin activity at sites of ECM attachment, possibly through the binding of a Src–EGFR complex to β1 integrin to promote Src activation at the plasma membrane. Phosphorylation of the EGFR on Tyr845 can lead to phosphorylation of p38MAPK and the downstream target Gab1 (Mueller et al., 2012). Taken together with the recent study by Rajadurai and colleagues (Rajadurai et al., 2012) that shows

Journal of Cell Science (2014) 127, 1712–1725 doi:10.1242/jcs.134734

that Gab1 directly interacts with cortactin to promote F-actin core formation, it is possible that integrin-induced activation of Src results in Src-mediated phosphorylation of the EGFR and cortactin to regulate the Gab1–cortactin interaction and subsequent F-actin remodeling during invadopodia formation.

Collectively, the data presented here demonstrate an important role for SNARE-mediated traffic in the formation of invadopodia during tumor cell invasion. This traffic is required for the transport of Src and the EGFR to sites of cell–ECM contact that contain β1 integrin. Furthermore, it is well established that Src has a key role in invadopodia formation through phosphorylation of cortactin, and we report that Src is also required for the phosphorylation of the EGFR. Our results not only provide insights into the molecular mechanisms of the early stages of cell invasion through the ECM but also suggest that the interaction between Src, EGFR and β1 integrin is a possible target for the development of therapies against malignancies with high expression levels of Src and the EGFR.

MATERIALS AND METHODS

Reagents and cDNA constructs

All chemicals were purchased from Sigma Chemical (St Louis, MO) or Fisher Scientific (Nepean, ON) unless otherwise indicated. Antibodies to the following proteins were obtained from the indicated suppliers: Src, Tyr418-phosphorylated Src, cortactin, FAK, β3 integrin, 58K Golgi (Applied Biological Materials); Tyr845-phosphorylated EGFR (Cell Signaling Technology); AIIB2, P4G11 β1 integrin, PC410 (Developmental Hybridoma Studies Bank); EGFR, β1 integrin clone K-20 (Santa Cruz Biotechnology); NSF (Enzo Life Sciences); SNAP23 (Abcam); syntaxin13 (Pierce). All secondary antibodies and Alexa-Fluor-647–phalloidin were purchased from Invitrogen.

The acylation motif of Lyn kinase fused to GFP (PM–GFP) was a kind gift from Tobias Meyer (Stanford University, Palo Alto, CA). Wild-type Src in the pUSEamp vector was provided by Nina Jones (University of Guelph, Guelph, ON). The membrane-targeted Src-CAAX construct was generated by PCR from the pUSEamp-SrcWT plasmid and cloned into pcDNA3.1(-). The following oligonucleotides were used as primers: forward (5′-ATAACTCGAGATGGGCAGCAACAAGAGC-3′), Src-CAAX reverse (5′-ATAAAAGAATTCTCACATAACTGTACACCTT-GTCCTTGATAGGTTCTCCCCGGGCTGGTACT-3′). Generation of pcDNA3.1 encoding the wild-type and mutant (E329Q-NSF) NSF constructs has been described elsewhere (Tayeb et al., 2005). Generation of GFP–SNAP23FL, GFP–SNAP23CΔ9, GFP–syntaxin13FL and GFP–syntaxin13cyto has been described elsewhere (Kean et al., 2009). β1 integrin knockdown was performed using human shRNA pRFP-C-RS ITGB1BP3 (Origene Technologies). Syntaxin13 knockdown was performed using SMARTpool ON-TARGETplus syntaxin13 siRNA and control siRNA (Dharmacon). SNAP23 knockdown was performed using shRNA control pLKO.1 and shRNA 144931 SNAP23 (Open Biosystems).

Cell culture and transfection

MDA-MB-231 and HT1080 cells were cultured in Dulbecco's modified Eagle's medium (DMEM) (Sigma-Aldrich) supplemented with 10% fetal bovine serum (Sigma-Aldrich) under 5% CO_2 at 37℃. Cells were transfected with PolyPlus transfection reagent (VWR International) as described by the manufacturer's protocol. All transfected constructs were expressed for 12–20 h. Cells were serum-starved overnight and plated onto 0.2%-gelatin coverslips or culture plates in serum-free medium and then treated with PP2 (10 μM), 11 nM AG1478 (EGFR inhibitor), β1 integrin inhibitory (10–30 μg/ml) or activation antibodies (20 μg/ml) where indicated.

Immunofluorescence microscopy

Cells were serum-starved overnight and plated on coverslips on 0.2% gelatin that had been labeled with Alexa Fluor 594, Alexa Fluor 488 or left unlabelled in serum-free medium. The cells and gelatin were subsequently fixed and permeabilized with 2% (w/v) paraformaldehyde in PBS and 0.2% Triton X-100 in PBS, respectively. Samples were blocked with 5% (w/v) bovine serum albumin (BSA) powder in PBS before staining with the primary and secondary antibodies. Samples were imaged using a 63× (NA 1.4) lens on a Leica DM-IRE2 upright microscope with a Leica TCS SP2 system (Leica, Heidelberg, Germany). Images were captured and 3D reconstructions were performed using the Leica Confocal Software package.

Image analysis

Localization of Src at the plasma membrane was assessed by using z-stacks of complete cells. Plasma membrane Src was determined as Src that had colocalized with the GFP-tagged acylation motif of Lyn kinase (Teruel et al., 1999). Total plasma membrane Src was manually selected and this, along with total Src, was measured using the particle-analysis function in ImageJ. Pearson's correlation and colocalization analysis were performed using the colocalization analysis plugin. All images were processed to remove noise and background, and the region of interest was manually selected for each image. Pearson's correlation for pixels where the intensity is greater than the threshold for both channels is represented, and values greater than 0.5 represent a biological correlation and an observed colocalization.

Co-immunoprecipitation

Cyanogen-bromide-activated sepharose beads (Sigma-Aldrich) were coated with antibody as per the manufacturer's instructions. Cells were lysed in 1% NP40, 2 mM EDTA, 10% glycerol, 137 mM NaCl, 20 mM Tris-HCl pH 8.0, 10 mM NaF, 10 mM $Na_4P_2O_7$, 0.2 mM Na_3VO_4 and protease inhibitor cocktail (Sigma). The lysate was incubated with antibody-bound beads overnight at 4℃, extensively washed and then eluted using 2.5× SDS running buffer. Alternatively, cell lysates were incubated with antibody for 4 h followed by the addition of ProteinG magnetic beads (New England Bioloabs) for 2 h, extensively washed and then eluted using 2.5× SDS running buffer. Proteins were separated using SDS-PAGE and analyzed by western blotting.

Cell-surface labeling and immunoprecipitation

Cells that had been cultured on 0.2% gelatin plates were rinsed with ice-cold PBS and incubated with PBS for 10 min at 4℃ on ice. 10 mM EZ-Link Sulfo-NHS-SS-Biotin (Thermo Scientific) in double-distilled H_2O was prepared immediately before use. Sulfo-NHS-Biotin in PBS was added at 4 ml (1 mM final concentration) per plate. The reaction was incubated for 2 h on ice. The cells were washed three times with ice-cold PBS, lysed and then immunoprecipitated with streptavidin beads. The lysate was incubated with the beads for 2 h at 4℃, washed and then eluted using 2.5× SDS running buffer with β-mercaptoethanol (2%). Proteins were separated using SDS-PAGE and analyzed by western blotting.

Cell invasion assay

Cell culture inserts, in 24-well dishes (CoStar), were prepared with fibronectin and Matrigel. The bottom chamber was coated with 20 μg/ml fibronectin and the upper chamber with 0.125 mg/ml growth factor reduced Matrigel (BD Biosciences). MDA-MB-231 cells or HT1080 cells were transfected for 2 h or left untransfected and serum-starved for 2 h, at which point they were lifted and seeded onto the Matrigel-coated upper surface in serum-free medium (80,000 cells/well). PP2 (10 μM) or 11 nM AG1478 (EGFR inhibitor) was added where indicated. The cells that invaded towards the chemoattractant (10% fetal bovine serum and 0.1% BSA) in the lower chamber and penetrated the Matrigel were fixed with 4% paraformaldehyde, stained with DAPI and counted. Cells that did not invade were removed with a cotton swab before fixation of samples. Ten fields of cells per membrane were counted. The data are presented as the number of cells that invaded through the Matrigel with the control (untreated sample set at 100%). For transfected cells, transfection efficiency was determined for each experiment using a control uncoated cell culture insert and used to determine cell invasion as a percentage of the transfected cells.

Invadopodia formation assay

Invadopodia formation was performed as previously described (Artym et al., 2009). Briefly, coverslips were coated with 5 mg/ml poly-L-lysine (Sigma-Aldrich), followed by 0.5% gluteraldehyde (Sigma-Aldrich) and inverted on an 80-µl drop of gelatin, incubated with 5 mg/ml sodium borohydride (Sigma-Aldrich) and then washed extensively with PBS. For immunoprecipitations, cell culture plates were coated in a similar manner.

Competing interests

The authors declare no competing interests.

Author contributions

K.C.W. performed all experiments, collected and analyzed data, prepared figures and drafted the manuscript. M.G.C. analyzed data, prepared figures and edited the manuscript.

Funding

This work was supported by the Natural Sciences and Engineering Research Council of Canada (NSERC). K.C.W. holds an NSERC Postgraduate Scholarship.

Supplementary material

Supplementary material available online at
http://jcs.biologists.org/lookup/suppl/doi:10.1242/jcs.134734/-/DC1

References

Aquino, G., Pannone, G., Santoro, A., Liguori, G., Franco, R., Serpico, R., Florio, G., De Rosa, A., Mattoni, M., Cozza, V. et al. (2012). pEGFR-Tyr 845 expression as prognostic factors in oral squamous cell carcinoma: a tissue-microarray study with clinic-pathological correlations. *Cancer Biol. Ther.* **13**, 967-977.

Artym, V. V., Zhang, Y., Seillier-Moiseiwitsch, F., Yamada, K. M. and Mueller, S. C. (2006). Dynamic interactions of cortactin and membrane type 1 matrix metalloproteinase at invadopodia: defining the stages of invadopodia formation and function. *Cancer Res.* **66**, 3034-3043.

Artym, V. V., Yamada, K. M. and Mueller, S. C. (2009). ECM degradation assays for analyzing local cell invasion. *Methods Mol. Biol.* **522**, 211-219.

Beaty, B. T., Sharma, V. P., Bravo-Cordero, J. J., Simpson, M. A., Eddy, R. J., Koleske, A. J. and Condeelis, J. (2013). β1 integrin regulates Arg to promote invadopodial maturation and matrix degradation. *Mol. Biol. Cell* **24**, 1661-1675, S1-S11.

Biscardi, J. S., Ishizawar, R. C., Silva, C. M. and Parsons, S. J. (2000). Tyrosine kinase signalling in breast cancer: epidermal growth factor receptor and c-Src interactions in breast cancer. *Breast Cancer Res.* **2**, 203-210.

Blouw, B., Seals, D. F., Pass, I., Diaz, B. and Courtneidge, S. A. (2008). A role for the podosome/invadopodia scaffold protein Tks5 in tumor growth in vivo. *Eur. J. Cell Biol.* **87**, 555-567.

Caswell, P. T., Chan, M., Lindsay, A. J., McCaffrey, M. W., Boettiger, D. and Norman, J. C. (2008). Rab-coupling protein coordinates recycling of alpha5beta1 integrin and EGFR1 to promote cell migration in 3D microenvironments. *J. Cell Biol.* **183**, 143-155.

Clark, E. S., Whigham, A. S., Yarbrough, W. G. and Weaver, A. M. (2007). Cortactin is an essential regulator of matrix metalloproteinase secretion and extracellular matrix degradation in invadopodia. *Cancer Res.* **67**, 4227-4235.

Clark, E. S., Brown, B., Whigham, A. S., Kochaishvili, A., Yarbrough, W. G. and Weaver, A. M. (2009). Aggressiveness of HNSCC tumors depends on expression levels of cortactin, a gene in the 11q13 amplicon. *Oncogene* **28**, 431-444.

Collins, R. F., Schreiber, A. D., Grinstein, S. and Trimble, W. S. (2002). Syntaxins 13 and 7 function at distinct steps during phagocytosis. *J. Immunol.* **169**, 3250-3256.

Dai, Q., Ling, Y. H., Lia, M., Zou, Y. Y., Kroog, G., Iwata, K. K. and Perez-Soler, R. (2005). Enhanced sensitivity to the HER1/epidermal growth factor receptor tyrosine kinase inhibitor erlotinib hydrochloride in chemotherapy-resistant tumor cell lines. *Clin. Cancer Res.* **11**, 1572-1578.

Desai, B., Ma, T. and Chellaiah, M. A. (2008). Invadopodia and matrix degradation, a new property of prostate cancer cells during migration and invasion. *J. Biol. Chem.* **283**, 13856-13866.

Destaing, O., Sanjay, A., Itzstein, C., Horne, W. C., Toomre, D., De Camilli, P. and Baron, R. (2008). The tyrosine kinase activity of c-Src regulates actin dynamics and organization of podosomes in osteoclasts. *Mol. Biol. Cell* **19**, 394-404.

Destaing, O., Planus, E., Bouvard, D., Oddou, C., Badowski, C., Bossy, V., Raducanu, A., Fourcade, B., Albiges-Rizo, C. and Block, M. R. (2010). β1A integrin is a master regulator of invadosome organization and function. *Mol. Biol. Cell* **21**, 4108-4119.

Eckert, M. A., Lwin, T. M., Chang, A. T., Kim, J., Danis, E., Ohno-Machado, L. and Yang, J. (2011). Twist1-induced invadopodia formation promotes tumor metastasis. *Cancer Cell* **19**, 372-386.

Garouniatis, A., Zizi-Sermpetzoglou, A., Rizos, S., Kostakis, A., Nikiteas, N. and Papavassiliou, A. G. (2012). FAK, CD44v6, c-Met and EGFR in colorectal cancer parameters: tumour progression, metastasis, patient survival and receptor crosstalk. *Int. J. Colorectal Dis.* **28**, 9-18.

Hirling, H., Steiner, P., Chaperon, C., Marsault, R., Regazzi, R. and Catsicas, S. (2000). Syntaxin 13 is a developmentally regulated SNARE involved in neurite outgrowth and endosomal trafficking. *Eur. J. Neurosci.* **12**, 1913-1923.

Huang, X., Sheu, L., Tamori, Y., Trimble, W. S. and Gaisano, H. Y. (2001). Cholecystokinin-regulated exocytosis in rat pancreatic acinar cells is inhibited by a C-terminus truncated mutant of SNAP-23. *Pancreas* **23**, 125-133.

Huck, L., Pontier, S. M., Zuo, D. M. and Muller, W. J. (2010). beta1-integrin is dispensable for the induction of ErbB2 mammary tumors but plays a critical role in the metastatic phase of tumor progression. *Proc. Natl. Acad. Sci. USA* **107**, 15559-15564.

Jorissen, R. N., Walker, F., Pouliot, N., Garrett, T. P., Ward, C. W. and Burgess, A. W. (2003). Epidermal growth factor receptor: mechanisms of activation and signalling. *Exp. Cell Res.* **284**, 31-53.

Kean, M. J., Williams, K. C., Skalski, M., Myers, D., Burtnik, A., Foster, D. and Coppolino, M. G. (2009). VAMP3, syntaxin-13 and SNAP23 are involved in secretion of matrix metalloproteinases, degradation of the extracellular matrix and cell invasion. *J. Cell Sci.* **122**, 4089-4098.

Kim, H. and Muller, W. J. (1999). The role of the epidermal growth factor receptor family in mammary tumorigenesis and metastasis. *Exp. Cell Res.* **253**, 78-87.

Linder, S. (2007). The matrix corroded: podosomes and invadopodia in extracellular matrix degradation. *Trends Cell Biol.* **17**, 107-117.

Mader, C. C., Oser, M., Magalhaes, M. A., Bravo-Cordero, J. J., Condeelis, J., Koleske, A. J. and Gil-Henn, H. (2011). An EGFR-Src-Arg-cortactin pathway mediates functional maturation of invadopodia and breast cancer cell invasion. *Cancer Res.* **71**, 1730-1741.

Mallard, F., Tang, B. L., Galli, T., Tenza, D., Saint-Pol, A., Yue, X., Antony, C., Hong, W., Goud, B. and Johannes, L. (2002). Early/recycling endosomes-to-TGN transport involves two SNARE complexes and a Rab6 isoform. *J. Cell Biol.* **156**, 653-664.

Meng, F. and Lowell, C. A. (1998). A beta 1 integrin signaling pathway involving Src-family kinases, Cbl and PI-3 kinase is required for macrophage spreading and migration. *EMBO J.* **17**, 4391-4403.

Mueller, S. C. and Chen, W. T. (1991). Cellular invasion into matrix beads: localization of beta 1 integrins and fibronectin to the invadopodia. *J. Cell Sci.* **99**, 213-225.

Mueller, K. L., Powell, K., Madden, J. M., Eblen, S. T. and Boerner, J. L. (2012). EGFR tyrosine 845 phosphorylation-dependent proliferation and transformation of breast cancer cells require activation of p38 MAPK. *Transl. Oncol.* **5**, 327-334.

Murphy, D. A. and Courtneidge, S. A. (2011). The 'ins' and 'outs' of podosomes and invadopodia: characteristics, formation and function. *Nat. Rev. Mol. Cell Biol.* **12**, 413-426.

Nakahara, H., Mueller, S. C., Nomizu, M., Yamada, Y., Yeh, Y. and Chen, W. T. (1998). Activation of beta1 integrin signaling stimulates tyrosine phosphorylation of p190RhoGAP and membrane-protrusive activities at invadopodia. *J. Biol. Chem.* **273**, 9-12.

O'Donovan, N. and Crown, J. (2007). EGFR and HER-2 antagonists in breast cancer. *Anticancer Res.* **27**, 1285-1294.

Onodera, Y., Nam, J. M., Hashimoto, A., Norman, J. C., Shirato, H., Hashimoto, S. and Sabe, H. (2012). Rab5c promotes AMAP1-PRKD2 complex formation to enhance β1 integrin recycling in EGF-induced cancer invasion. *J. Cell Biol.* **197**, 983-996.

Polgár, J., Chung, S. H. and Reed, G. L. (2002). Vesicle-associated membrane protein 3 (VAMP-3) and VAMP-8 are present in human platelets and are required for granule secretion. *Blood* **100**, 1081-1083.

Rajadurai, C. V., Havrylov, S., Zaoui, K., Vaillancourt, R., Stuible, M., Naujokas, M., Zuo, D., Tremblay, M. L. and Park, M. (2012). Met receptor tyrosine kinase signals through a cortactin-Gab1 scaffold complex, to mediate invadopodia. *J. Cell Sci.* **125**, 2940-2953.

Sato, K., Nagao, T., Iwasaki, T., Nishihira, Y. and Fukami, Y. (2003). Src-dependent phosphorylation of the EGF receptor Tyr-845 mediates Stat-p21waf1 pathway in A431 cells. *Genes Cells* **8**, 995-1003.

Scott, C. C., Furuya, W., Trimble, W. S. and Grinstein, S. (2003). Activation of store-operated calcium channels: assessment of the role of snare-mediated vesicular transport. *J. Biol. Chem.* **278**, 30534-30539.

Serio, R. N. (2012). Toward an integrative analysis of the tumor microenvironment in ovarian epithelial carcinoma. *Cancer Microenviron* **5**, 173-183.

Skalski, M., Yi, Q., Kean, M. J., Myers, D. W., Williams, K. C., Burtnik, A. and Coppolino, M. G. (2010). Lamellipodium extension and membrane ruffling require different SNARE-mediated trafficking pathways. *BMC Cell Biol.* **11**, 62.

Skalski, M., Sharma, N., Williams, K., Kruspe, A. and Coppolino, M. G. (2011). SNARE-mediated membrane traffic is required for focal adhesion kinase signaling and Src-regulated focal adhesion turnover. *Biochim. Biophys. Acta* **1813**, 148-158.

Soriano, P., Montgomery, C., Geske, R. and Bradley, A. (1991). Targeted disruption of the c-src proto-oncogene leads to osteopetrosis in mice. *Cell* **64**, 693-702.

Steffen, A., Le Dez, G., Poincloux, R., Recchi, C., Nassoy, P., Rottner, K., Galli, T. and Chavrier, P. (2008). MT1-MMP-dependent invasion is regulated by TI-VAMP/VAMP7. *Curr. Biol.* **18**, 926-931.

Tayeb, M. A., Skalski, M., Cha, M. C., Kean, M. J., Scaife, M. and Coppolino, M. G. (2005). Inhibition of SNARE-mediated membrane traffic impairs cell migration. *Exp. Cell Res.* **305**, 63-73.

Tehrani, S., Tomasevic, N., Weed, S., Sakowicz, R. and Cooper, J. A. (2007). Src phosphorylation of cortactin enhances actin assembly. *Proc. Natl. Acad. Sci. USA* **104**, 11933-11938.

Teruel, M. N., Blanpied, T. A., Shen, K., Augustine, G. J. and Meyer, T. (1999). A versatile microporation technique for the transfection of cultured CNS neurons. *J. Neurosci. Methods* **93**, 37-48.

Velling, T., Nilsson, S., Stefansson, A. and Johansson, S. (2004). beta1-Integrins induce phosphorylation of Akt on serine 473 independently of focal adhesion kinase and Src family kinases. *EMBO Rep.* **5**, 901-905.

von Minckwitz, G., Harder, S., Hövelmann, S., Jäger, E., Al-Batran, S. E., Loibl, S., Atmaca, A., Cimpoiasu, C., Neumann, A., Abera, A. et al. (2005). Phase I clinical study of the recombinant antibody toxin scFv(FRP5)-ETA specific for the ErbB2/HER2 receptor in patients with advanced solid malignomas. *Breast Cancer Res.* **7**, R617-R626.

Weaver, A. M. (2008). Cortactin in tumor invasiveness. *Cancer Lett.* **265**, 157-166.

Wennerberg, K., Armulik, A., Sakai, T., Karlsson, M., Fässler, R., Schaefer, E. M., Mosher, D. F. and Johansson, S. (2000). The cytoplasmic tyrosines of integrin subunit beta1 are involved in focal adhesion kinase activation. *Mol. Cell. Biol.* **20**, 5758-5765.

Whiteheart, S. W., Rossnagel, K., Buhrow, S. A., Brunner, M., Jaenicke, R. and Rothman, J. E. (1994). N-ethylmaleimide-sensitive fusion protein: a trimeric ATPase whose hydrolysis of ATP is required for membrane fusion. *J. Cell Biol.* **126**, 945-954.

Williams, K. C. and Coppolino, M. G. (2011). Phosphorylation of membrane type 1-matrix metalloproteinase (MT1-MMP) and its vesicle-associated membrane protein 7 (VAMP7)-dependent trafficking facilitate cell invasion and migration. *J. Biol. Chem.* **286**, 43405-43416.

Xu, Y., Martin, S., James, D. E. and Hong, W. (2002). GS15 forms a SNARE complex with syntaxin 5, GS28, and Ykt6 and is implicated in traffic in the early cisternae of the Golgi apparatus. *Mol. Biol. Cell* **13**, 3493-3507.

Yamaguchi, H., Lorenz, M., Kempiak, S., Sarmiento, C., Coniglio, S., Symons, M., Segall, J., Eddy, R., Miki, H., Takenawa, T. et al. (2005). Molecular mechanisms of invadopodium formation: the role of the N-WASP-Arp2/3 complex pathway and cofilin. *J. Cell Biol.* **168**, 441-452.

Zambonin-Zallone, A., Teti, A., Grano, M., Rubinacci, A., Abbadini, M., Gaboli, M. and Marchisio, P. C. (1989). Immunocytochemical distribution of extracellular matrix receptors in human osteoclasts: a beta 3 integrin is colocalized with vinculin and talin in the podosomes of osteoclastoma giant cells. *Exp. Cell Res.* **182**, 645-652.

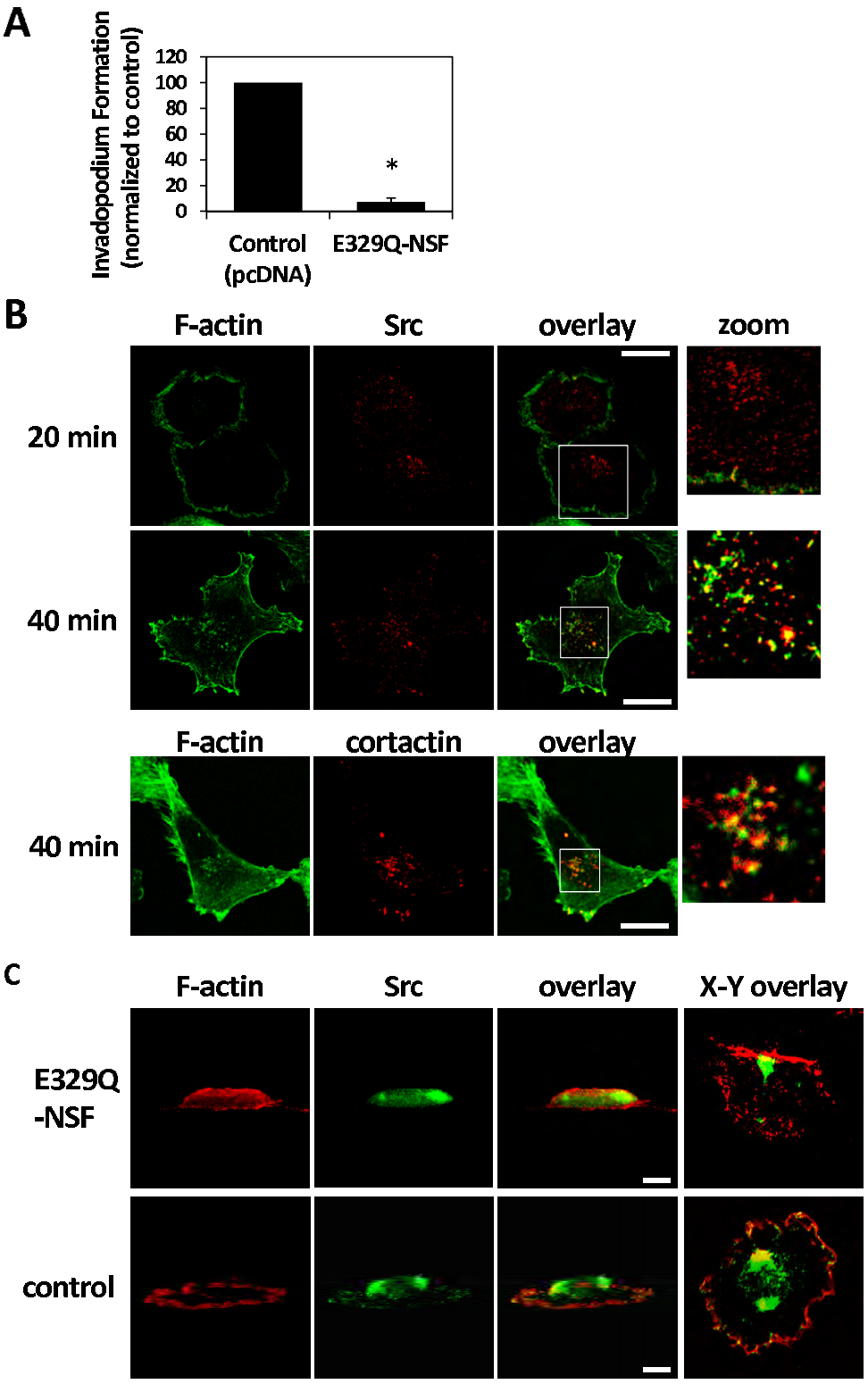

Fig. S1. SNARE-mediated membrane trafficking is required for invadopodium formation and Src trafficking. MDA-MB-231 cells were transfected with either E329Q-NSF or pcDNA3.1. (A) Cells were plated on coverslips coated with Alexa594-labeled gelatin for 5 hours, fixed, permeabilized, stained with anti-NSF antibody and phalloidin, and then F-actin-containing invadopodia were counted using a microscope. Means +/- SEM from 3 independent experiments in which 100 cells per sample were analyzed are shown. Asterisk denotes a value significantly different from wild-type cells; $p < 0.05$. (B) Cells were serum-starved, plated on gelatin-coated coverslips, fixed, permeabilized, and stained using anti-Src or anti-cortactin antibodies, followed by Alexa594-conjugated secondary antibody and Alexa488-phalloidin. Single confocal slices of the ventral membrane of cells are shown. Src co-localises with F-actin at the cell periphery at 20 and 40 mins. Actin/Src punctae are seen in the centre of the cell at 40min. At 40min, cortactin is also seen at F-actin punctae (bottom row). (C) Total Src localization in untransfected cells and cells transfected with E329Q-NSF for 12 hours, and plated on gelatin for 40min. Src is absent from the cell periphery (marked by F-actin staining) in cells expressing E329Q-NSF, compared to control cells. Scale bar = 10 μm.

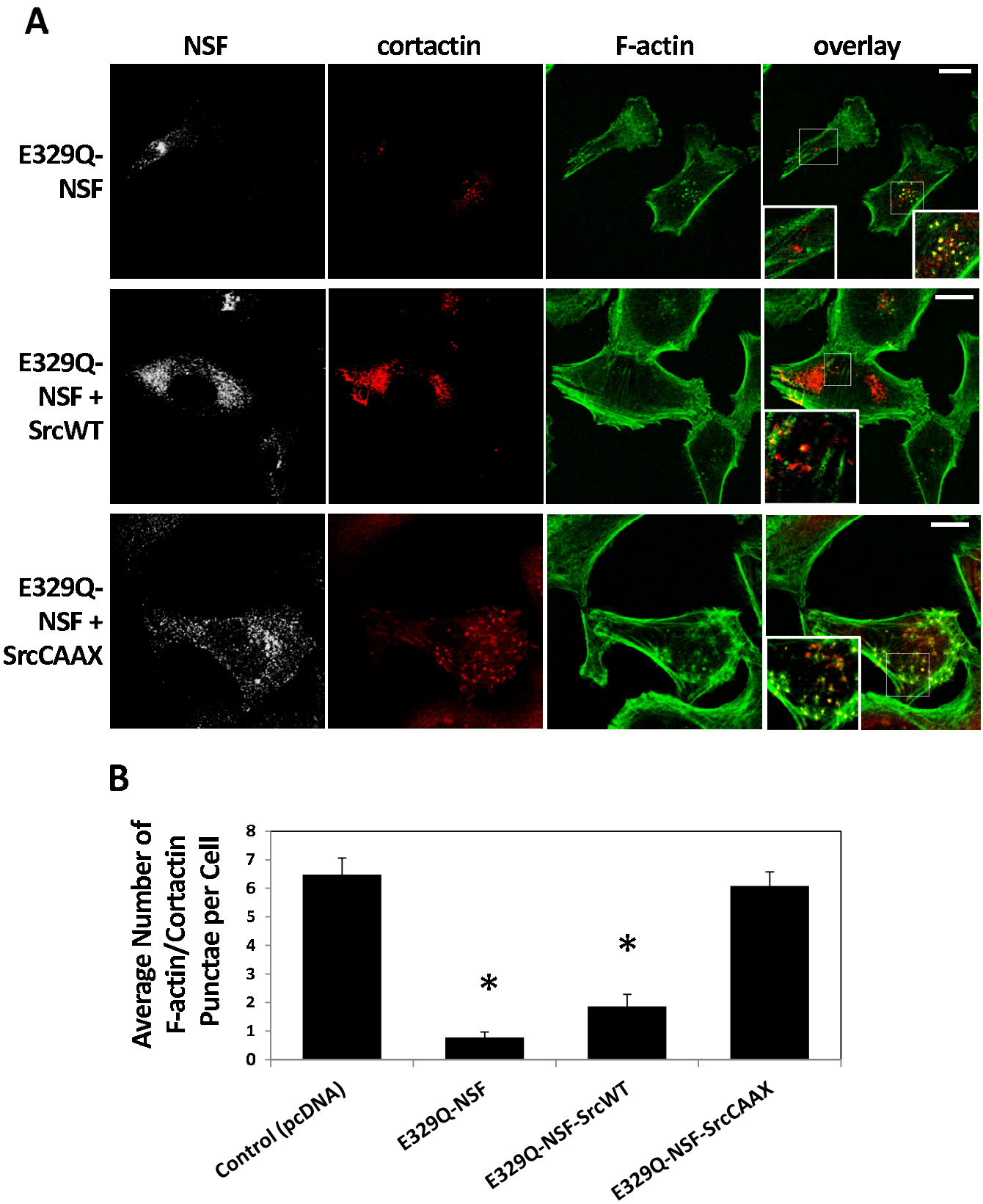

Fig. S2. Membrane-targeted Src restores invadopodia formation. MDA-MB-231 were co-transfected with E329Q-NSF along with either Src-WT or Src-CAAX. Cells were serum-starved, plated on gelatin for 40min, fixed, permeabilized, and stained for NSF, cortactin and F-actin. (A) Cells positive for transfected NSF are shown in the first column, and invadopodia are shown by the co-localization of F-actin and cortactin. E329Q-NSF-expressing cells (upper left cell in top panels) contain fewer F-actin/cortactin punctae than control cells (right-most cell in top panels). Expression of SrcCAAX, but not SrcWT, restores the formation of F-actin/cortactin-containing punctae. All images are single confocal slices at the level of the ventral membrane. Scale bar = 10μm. (B) Quantification of the number of F-actin/cortactin punctae per cell. Means +/- SEM from 3 independent experiments in which 30-50 cells per sample were analyzed are shown. Asterisk denotes a value significantly different from wild-type cells; $p < 0.05$.

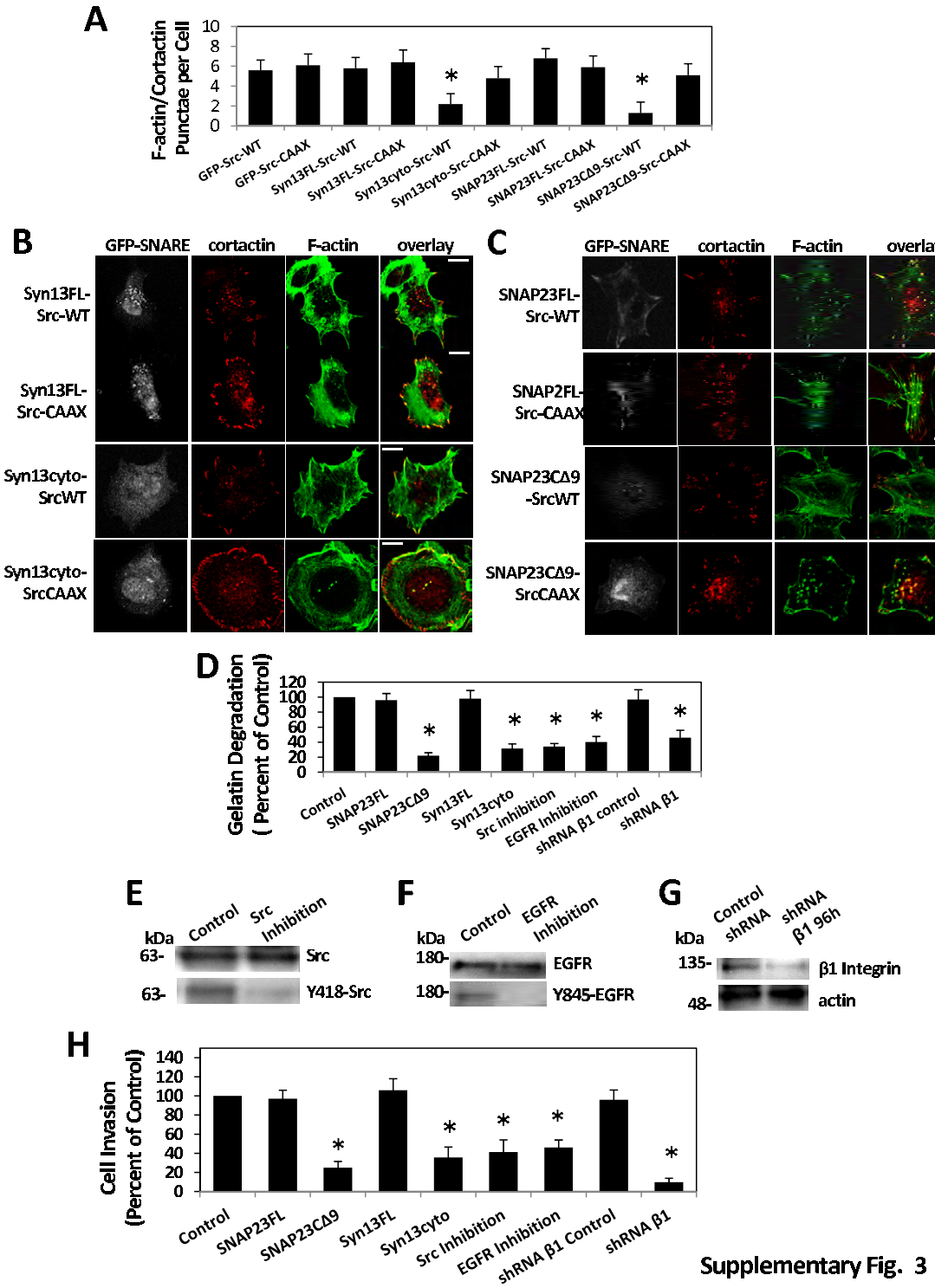

Fig. S3. Inhibition of SNAP23, Syntaxin13, Src, EGFR and β1 integrin impairs invadopodium formation, matrix degradation and invasion in HT-1080 cells. (A-C) Cells were cotransfected with GFP, GFP- SNAP23FL/CΔ9 or GFP-Syntaxin13FL/cyto and either Src-WT or Src-CAAX for 20 hrs. (A-C) Cells were serum starved overnight followed by culturing on gelatin coated coverslips for 40min in serum free media. Cells were fixed, permeabilized, and stained for anti-cortactin and actin (phalloidin). (A) Quantification of the number of actin/cortactin punctae demonstrate that invadopodia formation is rescued by Src-CAAX but not Src-WT. (B and C) Cells expressing Src-WT or Src-CAAX and, GFP-SNAP23FL/CΔ9, GFP-Syntaxin13FL/cyto, are represented in the first column in grey. Invadopodia formation is represented by co-localization of actin (green) and cortactin (red) in the overlay (yellow). (D and H) Cells were either transfected as in (A) or treated with 10μM PP2 (Src inhibitor), 11nM AG1478 (EGFR inhibitor)or transfected with shRNA control or shRNA β1 integrin. (D) Cells were plated on Alexa594-labeled gelatin for 3 hrs and scored as for presence or absence of matrix degradation. (E) Cells were treated with PP2, lysed and Western blotted for Y418-Src, stripped and reprobed for Src. (F) Cells were treated with AG1478, lysed and Western blotted for Y845-EGFR, stripped and reprobed for EGFR. (G) shRNA control and shRNA β1 integrin transfected cells were lysed 96hrs post transfection and probed for total β1 integrin; actin represents a loading control. (H) Cells were collected and subjected to transwell invasion assay. Cells invaded through matrigel towards 10% FBS for 18 hours and were then fixed and counted. Asterisk denotes a value significantly different from control cells ($p < 0.05$).